Geosci. Model Dev., 16, 6187–6209, 2023
https://doi.org/10.5194/gmd-16-6187-2023

Geoscientific Model Development
Open Access
EGU

Description and evaluation of the new UM–UKCA (vn11.0) Double Extended Stratospheric–Tropospheric (DEST vn1.0) scheme for comprehensive modelling of halogen chemistry in the stratosphere

Ewa M. Bednarz[1,a,b], **Ryan Hossaini**[1,2], **N. Luke Abraham**[3,4], **and Martyn P. Chipperfield**[5,6]

[1]Lancaster Environment Centre, Lancaster University, Lancaster, UK
[2]Centre of Excellence in Environmental Data Science, Lancaster University, Lancaster, UK
[3]Department of Chemistry, University of Cambridge, Cambridge, UK
[4]National Centre for Atmospheric Science (NCAS), Cambridge, UK
[5]School of Earth and Environment, University of Leeds, Leeds, UK
[6]National Centre for Earth Observation (NCEO), University of Leeds, Leeds, UK
[a]now at: Cooperative Institute for Research in Environmental Sciences (CIRES), University of Colorado Boulder, Boulder, CO, USA
[b]now at: NOAA Chemical Sciences Laboratory (NOAA CSL), Boulder, CO, USA

Correspondence: Ewa M. Bednarz (ewa.bednarz@noaa.gov)

Received: 30 August 2022 – Discussion started: 15 December 2022
Revised: 1 August 2023 – Accepted: 24 August 2023 – Published: 2 November 2023

Abstract. The paper describes the development and performance of the Double Extended Stratospheric–Tropospheric (DEST vn1.0) chemistry scheme, which forms a part of the Met Office's Unified Model coupled to the United Kingdom Chemistry and Aerosol (UM–UKCA) chemistry–climate model, which is the atmospheric composition model of the United Kingdom Earth System Model (UKESM). The scheme extends the standard Stratospheric–Tropospheric chemistry scheme (StratTrop) by including a range of important updates to the halogen chemistry. These allow process-oriented studies of stratospheric ozone depletion and recovery, including the impacts from both controlled long-lived ozone-depleting substances (ODSs) and emerging issues around uncontrolled very short-lived substances (VSLS). The main updates in DEST are (i) an explicit treatment of 14 of the most important long-lived ODSs; (ii) an inclusion of brominated VSLS (Br-VSLS) emissions and chemistry; and (iii) an inclusion of chlorinated VSLS (Cl-VSLS) emissions/LBCs (lower boundary conditions) and chemistry. We evaluate the scheme's performance by comparing DEST simulations against analogous runs made with the standard StratTrop scheme and against observational and reanalysis datasets. Overall, our scheme addresses some significant shortcomings in the representation of atmospheric halogens in the standard StratTrop scheme and will thus be particularly relevant for studies of ozone layer recovery and processes affecting it, in support of future World Meteorological Organization (WMO) Ozone Assessment Reports.

1 Introduction

The last 2 decades have seen extensive international efforts dedicated to the development and application of complex chemistry–climate models (CCMs) and Earth system models (ESMs). By explicitly simulating the interplay of atmospheric chemistry, circulation, and the radiative balance of the atmosphere, these models have proved very useful in addressing a range of coupled composition–climate problems of environmental significance, including, for example, how climate change might impact air quality (e.g. Turnock et al., 2020) and how the stratospheric ozone layer might evolve under a range of potential climate scenarios (e.g. Dhomse et al., 2018). One of the main CCMs developed and used in the United Kingdom is the UK Met Office's Unified Model coupled to the United Kingdom Chemistry and Aerosol model

(UM–UKCA; Morgenstern et al., 2009; O'Connor et al., 2014; Archibald et al., 2020). When coupled to an interactive ocean, sea ice, and terrestrial and oceanic biochemistry modules, the model has also been recently known as United Kingdom Earth System Model (UKESM1; Sellar et al., 2019). It currently includes a comprehensive Stratospheric–Tropospheric chemistry scheme (StratTrop; Archibald et al., 2020) suitable for addressing a wide range of chemistry–climate problems.

Depletion of the stratospheric ozone layer is one of the most prominent environmental issues of the last several decades. While the Montreal Protocol and its amendments are successfully reducing the atmospheric abundance of halogenated long-lived ozone-depleting substances (ODSs), and thus ozone recovery is expected this century (e.g. Dhomse et al., 2018), challenges to our understanding of stratospheric composition, along with potential challenges for the Montreal Protocol, have recently emerged. These include (1) a persistent downward trend in the extra-polar lower-stratospheric ozone (e.g. Ball et al., 2019); (2) illicit production of certain controlled chlorofluorocarbons (CFCs; e.g. Montzka et al., 2018); and (3) increasing emissions of uncontrolled halogenated very short-lived substances (VSLS), such as dichloromethane, CH_2Cl_2, and chloroform, $CHCl_3$ (e.g. Fang et al., 2019; Hossaini et al., 2019; Claxton et al., 2020). These issues, among others, are areas of active stratospheric research that are relevant to understanding the expected timescale of ozone recovery and the direct and indirect climate impacts of ODSs.

The current generation of state-of-the-art CCMs should be equipped to examine topical issues in stratospheric composition research. However, the StratTrop scheme of UKESM1 is not optimised for this purpose, as it does not currently include an explicit representation of most long-lived halogenated ODSs. Instead, total chlorine and bromine contributions from these are "lumped" into three main "surrogate" ODS species. Historically, such an approach has been adopted in some CCMs when balancing the need for a reasonable simulation of the stratosphere against the added computational burden of a more complex chemistry scheme that includes a large number of advected tracers. While the lumping approach constitutes a useful approximation of total stratospheric halogen content, it may not produce a fully correct time evolution of halogenated source and product gases that is needed in studies where stratospheric ozone is the primary focus. Notably, an Extended Stratospheric Chemistry scheme (CheS+; Bednarz et al., 2016), which included an explicit treatment of 12 long-lived ODSs but no tropospheric chemistry, was available in an older UM–UKCA model version (vn7.3) that participated in phase 1 of the Chemistry–Climate Model Initiative project (CCMI-1; Eyring et al., 2013) in support of the 2018 World Meteorological Organization (WMO) and United Nations Environment Programme (UNEP) Ozone Assessment Report (WMO, 2018). However, the scheme has not yet been incorporated into the newer UM–UKCA/UKESM versions that include other important improvements. Both the recent CMIP6 (i.e. phase 6 of the Climate Model Intercomparison Project) UKESM1 simulations (Sellar et al., 2020) and the most recent CCMI-2022 (i.e. phase 2 of CCMI, Plummer et al., 2021) UKESM1 simulations in support of the 2022 WMO and UNEP Ozone Assessment Report still use the simplified halogen lumping approach of the StratTrop scheme (Archibald et al., 2020).

In addition to longer-lived ODSs, recent studies have showed the importance of chlorinated and brominated very short-lived substances (Cl-VSLS and Br-VSLS) in contributing to the total halogen budget and, thus, potentially playing an important role in modulating the evolution of stratospheric ozone (e.g. Fernandez et al., 2017; Hossaini et al., 2019; Bednarz et al., 2022). Prominent Cl-VSLS include dichloromethane and chloroform, both of which have significant anthropogenic sources (Chipperfield et al., 2020). Importantly, Cl-VSLS are not yet included in the standard StratTrop scheme of UKESM1. The stratospheric bromine contribution from Br-VSLS, on the other hand, is only roughly approximated in StratTrop by including an extra 5 ppt (parts per trillion) of bromine to the lumped lower boundary condition (LBC) of the surrogate gas, methyl bromide (CH_3Br). Fernandez et al. (2021) performed a detailed set of sensitivity experiments with the CAM-Chem (Community Atmosphere Model with Chemistry) chemistry–climate model to investigate the impact of this surrogate approach versus a fully explicit scheme (i.e. with individual VSLS tracers emitted at the surface). Their results highlighted that the latter approach leads to a greater amount of inorganic bromine and ozone destruction in the extra-polar lowermost stratosphere – a region where ozone changes exert relatively large radiative effects (e.g. Hossaini et al., 2015). Wales et al. (2018) also showed that an explicit treatment of Br-VSLS is important for correctly simulating the distribution of bromine compounds in the lower stratosphere and thus that models relying on the surrogate approach may potentially underestimate bromine-catalysed ozone loss in the region.

Here we describe the development and evaluation of the Double Extended Stratospheric–Tropospheric (DEST vn1.0) chemistry scheme of UM–UKCA (currently at version 11.0). The DEST scheme addresses the above-described shortcomings in the representation of halogen processes in the standard StratTrop scheme of UM–UKCA/UKESM1 (Archibald et al., 2020), including (i) an explicit treatment of 14 most important long-lived ODSs; (ii) an inclusion of Br-VSLS emissions and chemistry; and (iii) an inclusion of Cl-VSLS emissions/LBCs and chemistry. Section 3 provides a detailed account of the chemistry scheme improvements. Section 4.1 describes the experiments performed to evaluate the performance of DEST, and Sect. 4.2–4.3 assess the DEST results against the results of analogous simulations performed with the standard StratTrop scheme and observations or reanalysis. A summary, along with a discussion and outlook, is presented in Sect. 5.

2 The UM–UKCA model

We use version 11.0 of the UM–UKCA chemistry–climate model, the atmosphere-only configuration similar to the UKESM1 Earth system model (Sellar et al., 2019). The full description of the model can be found in Archibald et al. (2020). Briefly, the model consists of the Global Atmosphere 7.1 configuration of the version 3 of the Hadley Centre Global Environment Model (GA7.1 HadGEM3; Walters et al., 2019) coupled to the UKCA chemistry and aerosol module (Morgenstern et al., 2009). The latter includes the Global Model of Aerosol Processes (GLOMAP-mode) aerosol microphysics module (Mann et al., 2010; Mulcahy et al., 2018, 2020) and the fully interactive Fast-JX photolysis scheme covering the wavelength range of 177–850 nm (Telford et al., 2013) up to 0.2 hPa altitude and the lookup tables (Lary and Pyle, 1991) above. The horizontal resolution of the model used here is 1.875° longitude × 1.75° latitude, with 85 vertical levels up to ∼ 84 km on a terrain-following hybrid height coordinate.

3 Chemistry scheme improvements in DEST

The standard UM–UKCA/UKESM1 StratTrop chemistry scheme is described and evaluated in Archibald et al. (2020). The DEST scheme extends the StratTrop (vn11.0) scheme by incorporating important improvements to the representation of halogen processes. These are described below. A list of all halogenated tracers in DEST is shown in Table 1.

3.1 Unlumping of long-lived ODSs

The standard StratTrop scheme explicitly represents only three halogen source gases, namely $CFCl_3$ (CFC-11), CF_2Cl_2 (CFC-12), and CH_3Br. In order to reflect the changes in the total stratospheric halogen content, whose evolution is, by and large, controlled by the Montreal Protocol and its subsequent amendments, the imposed globally uniform LBCs (lower boundary conditions) for these species include halogen contributions from many other major longer-lived ODSs. In particular, CFC-11 acts as a surrogate for the chlorine contributions from CCl_4, CH_3CCl_3, HCFC-141b, HCFC142-b, Halon-1211, and CH_3Cl; CFC-12 acts as a surrogate for chlorine from CFC-113, CFC-114, CFC-115, and HCFC-22; and CH_3Br acts as a surrogate for bromine from Halon-1211, Halon-1301, Halon-1202, and Halon-2402. As discussed in the Introduction, this lumped halogen approach, while providing a reasonable approximation of the total stratospheric chlorine and bromine content, is unlikely to accurately represent the evolution of halogenated source and product gases of importance to stratospheric ozone.

To assist future modelling efforts examining, for instance, stratospheric ozone recovery, DEST includes explicit treatment of 14 of the most important ODSs, namely CFC-11, CFC-12, CFC-113, CFC-114, CFC-115, CH_3Cl, CCl_4, CH_3CCl_3, HCFC-22, HCFC-141b, HCFC-142b, CH_3Br, Halon-1211, and Halon-1301 (Table 1). The model's time-varying surface concentrations of these gases are controlled using globally uniform prescribed LBCs. For Halon-1301, the LBCs include also the lumped bromine atom contributions from Halon-1202 and Halon-2402. This approach is similar to the older Extended Stratospheric Chemistry (CheS+) scheme used in Bednarz et al. (2016) but with even more unlumped ODS tracers. In particular, DEST includes CFC-114, CFC-115, HCFC-141b, and HCFC-142b, as well as lumping of Halon-1202 and Halon-2402 onto Halon-1301, which were not included in the older CheS+ scheme.

3.2 Inclusion of Br-VSLS

Wales et al. (2018) and Fernandez et al. (2021) highlighted the importance of including spatially varying Br-VSLS emissions in models, as opposed to LBCs, for the correct representation of tropospheric bromine and its transport to the stratosphere. The standard StratTrop UM–UKCA scheme does not include an explicit representation of Br-VSLS, although their contribution to the total bromine budget is approximated by adding an extra 5 ppt bromine to the LBCs of CH_3Br.

In contrast, our new DEST scheme includes the explicit treatment of five of the most important naturally emitted Br-VSLS, namely bromoform ($CHBr_3$); dibromomethane (CH_2Br_2); bromochloromethane (CH_2BrCl); dibromochloromethane ($CHBr_2Cl$); and bromodichloromethane ($CHBrCl_2$). The tropospheric abundance of these species now evolves according to prescribed spatially and monthly varying emission fluxes, which are based on the climatological emission inventories developed by Ordóñez et al. (2012). The annual mean global total emissions for each species are given in Table 2. Note that these values are slightly smaller than the yearly mean values reported in Ordóñez et al. (2012) because of the 360 d calendar used in the default free-running configuration of UM–UKCA. Once emitted, the Br-VSLS tracers can react with OH, $O(^1D)$, and Cl (Table 3), as well as undergo photolysis to release inorganic bromine (Table 4).

3.3 Inclusion of Cl-VSLS, including $COCl_2$ chemistry

StratTrop does not include any Cl-VSLS chemistry. In contrast, DEST includes the explicit treatment of four of the most important Cl-VSLS, namely dichloromethane (CH_2Cl_2); chloroform ($CHCl_3$); perchloroethylene (C_2Cl_4); and ethylene dichloride ($C_2H_4Cl_2$). The atmospheric concentrations of these species are constrained at the surface using either LBC or, for CH_2Cl_2 and C_2Cl_4, spatially varying emission fluxes. The former approach is used in this evaluation (Sect. 4) and in the recent study of Bednarz et al. (2022). The surface lower boundary conditions for each Cl-VSLS are applied in the model in five latitude bands (90–30° S, 30–0° S,

Table 1. Summary of the halogen tracers included in DEST. New species added in DEST that are absent in the standard StratTrop scheme are highlighted in bold. Note that in StratTrop, CFC11, CFC12, and CH_3Br constitute surrogate species reflecting lumped halogen contributions from other long-lived ODSs (see Sect. 3.1 for details).

Species type	Species formula
Cl_y	Cl, **Cl_2**, Cl_2O_2, ClO, OClO, HCl, HOCl, $ClONO_2$, **$ClNO_2$**
Br_y	Br, **Br_2**, BrO, $BrONO_2$, HBr, HOBr
Mixed Cl_y / Br_y	BrCl
Long-lived ODSs	$CFCl_3$ (CFC11), CF_2Cl_2 (CFC12), **$CF_2ClCFCl_2$ (CFC113)**, **CF_2ClCF_2Cl (CFC114)**, **CF_2ClCF_3 (CFC115)**, **CH_3Cl**, **CCl_4**, **CH_3CCl_3**, **CHF_2Cl (HCFC22)**, **CH_3CFCl_2 (HCFC141b)**, **CH_3CF_2Cl (HCFC142b)**, CH_3Br, **CF_2ClBr (Halon-1211)**, **CF_3Br (Halon-1301)**
Br-VSLS	**$CHBr_3$**, **CH_2Br_2**, **CH_2BrCl**, **$CHBr_2Cl$**, **$CHBrCl_2$**
Cl-VSLS	**CH_2Cl_2**, **$CHCl_3$**, **C_2Cl_4**, **$C_2H_4Cl_2$**
Organic mid products	**$COCl_2$**, **$CHCl_2O_2$**

Table 2. Annual mean global total emissions of Br-VSLS imposed in the model, based on the inventory of Ordóñez et al. (2012).

Species	Total emissions ($Gg\,yr^{-1}$)
$CHBr_3$	528
CH_2Br_2	67
CH_2BrCl	10
$CHBr_2Cl$	20
$CHBrCl_2$	22

0–30° N, 30–60° N, and 60–90° N), based on the National Oceanic and Atmospheric Administration (NOAA) and Advanced Global Atmospheric Gases Experiment (AGAGE) surface monitoring data, and vary annually. Once in the atmosphere, these Cl-VSLS tracers may undergo photolysis (Table 4) and bimolecular reactions with OH and Cl (Table 3). C_2Cl_4 is also subject to a termolecular reaction with Cl atoms (Table 5), a reaction shown to improve model measurement agreement of C_2Cl_4 profiles in the tropical upper troposphere (Hossaini et al., 2019).

Two organic products following the atmospheric degradation of Cl-VSLS are included, namely a short-lived peroxy species $CHCl_2O_2$ and phosgene ($COCl_2$). $CHCl_2O_2$ is produced from the reaction of CH_2Cl_2 with OH or Cl; it can then react with NO, NO_3, HO_2, or CH_3O_2 (Table 3) or undergo photolysis (Table 4). $COCl_2$ is produced from the reactions of CH_2Cl_2 and $CHCl_3$ with Cl and from the reaction of C_2Cl_4 with OH. These intermediate organic chlorine species, particularly $COCl_2$, are longer lived than inorganic product gases; this can thus effectively increase the lifetime of atmospheric chlorine and facilitate its transport into the lower stratosphere.

Apart from Cl-VSLS, $COCl_2$ is also produced in the atmosphere from the photolysis of long-lived CCl_4 (Table 4) and from the reaction of CH_3CCl_3 with OH (Table 3). Assuming this contribution to atmospheric $COCl_2$ from the longer-lived ODSs is properly accounted for, observed $COCl_2$ can be used to help infer the stratospheric product injection of chlorine resulting from Cl-VSLS emissions (Harrison et al., 2019). In DEST, $COCl_2$ is lost via photolysis, reaction with $O(^1D)$, and wet and dry deposition.

3.4 Further updates and improvements

A number of other improvements to the halogen chemistry scheme are included in DEST. First, in addition to the new tracers described in Sect. 3.1–3.3, the scheme also includes Cl_2, Br_2, and $ClNO_2$ as new inorganic halogen tracers (Table 1). These tracers are important products of heterogenous reactions that occur on polar stratospheric clouds (PSCs) and sulfate aerosols (Table 6) but are otherwise not explicitly included in StratTrop. The rates of all bimolecular halogen reactions in DEST have been updated to the Jet Propulsion Laboratory (JPL, 2015) values, and a number of reactions or reaction channels including the newly added Cl_2, Br_2, and $ClNO_2$ tracers have been added (Tables 3, 5, and 6).

Regarding the model deposition processes, in addition to the wet deposition of HCl, HOCl, $ClONO_2$, HBr, HOBr, and $BrONO_2$ found in standard StratTrop, we have also included the wet deposition of Cl, ClO, Cl_2, $ClNO_2$, Br, Br_2 and BrCl in DEST, using Henry's law constants from Sander (2015), with the exception of $ClNO_2$, which uses the value from Ordóñez et al. (2012). Regarding dry deposition, DEST includes the dry deposition of $ClONO_2$ and $BrONO_2$, in addition to the HCl, HOCl, HBr, and HOBr already included in StratTrop.

Table 3. Summary of bimolecular reactions of atmospheric halogens included in DEST. Reactions and/or channels absent in the standard StratTrop scheme are highlighted in bold. Unless stated otherwise, all rate constants have been updated to reflect the information in Burkholder et al. (2015).

Reactants	Products	Rate constant	Source
$Br + Cl_2O_2$	$\rightarrow BrCl + Cl + O_2$	$5.90 \times 10^{-12} \cdot \exp(-170/T)$	Burkholder et al. (2015)
$Br + HCHO$	$\rightarrow HBr + CO + HO_2$	$1.70 \times 10^{-11} \cdot \exp(-800/T)$	Burkholder et al. (2015)
$Br + HO_2$	$\rightarrow HBr + O_2$	$4.80 \times 10^{-12} \cdot \exp(-310/T)$	Burkholder et al. (2015)
$Br + O_3$	$\rightarrow BrO + O_2$	$1.60 \times 10^{-11} \cdot \exp(-780/T)$	Burkholder et al. (2015)
$Br + OClO$	$\rightarrow BrO + ClO$	$2.60 \times 10^{-11} \cdot \exp(-1300/T)$	Burkholder et al. (2015)
$BrO + BrO$	$\rightarrow Br + Br + O_2$ $\rightarrow \mathbf{Br_2 + O_2}$	$2.40 \times 10^{-12} \cdot \exp(40/T)$ $2.80 \times 10^{-14} \cdot \exp(860/T)$	Burkholder et al. (2015)
$BrO + ClO$	$\rightarrow Br + Cl + O_2$ $\rightarrow Br + OClO$ $\rightarrow BrCl + O_2$	$2.30 \times 10^{-12} \cdot \exp(260/T)$ $9.50 \times 10^{-13} \cdot \exp(550/T)$ $4.10 \times 10^{-13} \cdot \exp(290/T)$	Burkholder et al. (2015)
$BrO + HO_2$	$\rightarrow HOBr + O_2$	$4.50 \times 10^{-12} \cdot \exp(460/T)$	Burkholder et al. (2015)
$BrO + NO$	$\rightarrow Br + NO_2$	$8.80 \times 10^{-12} \cdot \exp(260/T)$	Burkholder et al. (2015)
$BrO + OH$	$\rightarrow Br + HO_2$	$1.70 \times 10^{-11} \cdot \exp(250/T)$	Burkholder et al. (2015)
$CF_2Cl_2 + O(^1D)$	$\rightarrow Cl + ClO$	$1.20 \times 10^{-10} \cdot \exp(25/T)$	Burkholder et al. (2015)
$CFCl_3 + O(^1D)$	$\rightarrow Cl + Cl + ClO$	2.07×10^{-10}	Burkholder et al. (2015)
$Cl + CH_4$	$\rightarrow HCl + CH_3O_2$	$7.10 \times 10^{-12} \cdot \exp(-1270/T)$	Burkholder et al. (2015)
$Cl + Cl_2O_2$	$\rightarrow 3 \cdot Cl$	$7.60 \times 10^{-11} \cdot \exp(65/T)$	Burkholder et al. (2015)
$Cl + ClONO_2$	$\rightarrow 2 \cdot Cl + NO_3$	$6.50 \times 10^{-12} \cdot \exp(135/T)$	Burkholder et al. (2015)
$Cl + H_2$	$\rightarrow HCl + H$	$3.05 \times 10^{-11} \cdot \exp(-2270/T)$	Burkholder et al. (2015)
$Cl + H_2O_2$	$\rightarrow HCl + HO_2$	$1.10 \times 10^{-11} \cdot \exp(-980/T)$	Burkholder et al. (2015)
$Cl + HCHO$	$\rightarrow HCl + CO + HO_2$	$8.10 \times 10^{-11} \cdot \exp(-30/T)$	Burkholder et al. (2015)
$Cl + HO_2$	$\rightarrow ClO + OH$ $\rightarrow HCl + O_2$	$3.60 \times 10^{-11} \cdot \exp(-375/T)$ $1.40 \times 10^{-11} \cdot \exp(270/T)$	Burkholder et al. (2015)
$Cl + HOCl$	$\rightarrow 2 \cdot Cl + OH$	$3.40 \times 10^{-12} \cdot \exp(-130/T)$	Burkholder et al. (2015)
$Cl + MeOOH$	$\rightarrow HCl + CH_3O_2$	5.70×10^{-11}	Burkholder et al. (2015)
$Cl + NO_3$	$\rightarrow ClO + NO_2$	2.40×10^{-11}	Burkholder et al. (2015)
$Cl + O_3$	$\rightarrow ClO + O_2$	$2.30 \times 10^{-11} \cdot \exp(-200/T)$	Burkholder et al. (2015)
$Cl + OClO$	$\rightarrow 2 \cdot ClO$	$3.40 \times 10^{-11} \cdot \exp(160/T)$	Burkholder et al. (2015)
$ClO + ClO$	$\rightarrow \mathbf{Cl_2 + O_2}$ $\rightarrow \mathbf{Cl_2 + O_2}$ $\rightarrow Cl + OClO$	$1.00 \times 10^{-12} \cdot \exp(-1590/T)$ $3.00 \times 10^{-11} \cdot \exp(-2450/T)$ $3.50 \times 10^{-13} \cdot \exp(-1370/T)$	Burkholder et al. (2015)
$ClO + HO_2$	$\rightarrow HOCl + O_2$	$2.60 \times 10^{-12} \cdot \exp(290/T)$	Burkholder et al. (2015)
$ClO + MeOO$	$\rightarrow Cl + HCHO + HO_2$	$1.80 \times 10^{-12} \cdot \exp(-600/T)$	Burkholder et al. (2015)
$ClO + NO$	$\rightarrow Cl + NO_2$	$6.40 \times 10^{-12} \cdot \exp(290/T)$	Burkholder et al. (2015)
$ClO + NO_3$	$\rightarrow Cl + O_2 + NO_2$	4.70×10^{-13}	Burkholder et al. (2015)
$CH_3Br + Cl$	$\rightarrow Br + HCl$	$1.46 \times 10^{-11} \cdot \exp(-1040/T)$	Burkholder et al. (2015)
$CH_3Br + O(^1D)$	$\rightarrow Br + OH$	1.80×10^{-10}	Burkholder et al. (2015)
$CH_3Br + OH$	$\rightarrow Br + H_2O$	$1.42 \times 10^{-12} \cdot \exp(-1150/T)$	Burkholder et al. (2015)

Table 3. Continued.

Reactants	Products	Rate constant	Source
$Br + NO_3$	$\rightarrow BrO + NO_2$	1.60×10^{-11}	Burkholder et al. (2015)
$HBr + O(^1D)$	$\rightarrow HBr + O(^3P)$ $\rightarrow OH + Br$ $\rightarrow \mathbf{H + BrO}$	3.00×10^{-11} 9.00×10^{-11} 3.00×10^{-11}	Burkholder et al. (2015)
$HCl + O(^1D)$	$\rightarrow H + ClO$ $\rightarrow O(^3P) + HCl$ $\rightarrow OH + Cl$	3.30×10^{-11} 1.80×10^{-11} 9.90×10^{-11}	Burkholder et al. (2015)
$BrO + O(^3P)$	$\rightarrow O_2 + Br$	$1.90 \times 10^{-11} \cdot \exp(230/T)$	Burkholder et al. (2015)
$ClO + O(^3P)$	$\rightarrow Cl + O_2$	$2.80 \times 10^{-11} \cdot \exp(85/T)$	Burkholder et al. (2015)
$ClONO_2 + O(^3P)$	$\rightarrow ClO + NO_3$	$3.60 \times 10^{-12} \cdot \exp(-840/T)$	Burkholder et al. (2015)
$HBr + O(^3P)$	$\rightarrow OH + Br$	$5.80 \times 10^{-12} \cdot \exp(-1500/T)$	Burkholder et al. (2015)
$HCl + O(^3P)$	$\rightarrow OH + Cl$	$1.00 \times 10^{-11} \cdot \exp(-3300/T)$	Burkholder et al. (2015)
$HOCl + O(^3P)$	$\rightarrow OH + ClO$	1.70×10^{-13}	Burkholder et al. (2015)
$OClO + O(^3P)$	$\rightarrow O_2 + ClO$	$2.40 \times 10^{-12} \cdot \exp(-960/T)$	Burkholder et al. (2015)
$ClO + OH$	$\rightarrow HCl + O_2$ $\rightarrow HO_2 + Cl$	$6.00 \times 10^{-13} \cdot \exp(230/T)$ $7.40 \times 10^{-12} \cdot \exp(270/T)$	Burkholder et al. (2015)
$ClONO_2 + OH$	$\rightarrow HOCl + NO_3$	$1.20 \times 10^{-12} \cdot \exp(-330/T)$	Burkholder et al. (2015)
$HCl + OH$	$\rightarrow H_2O + Cl$	$1.80 \times 10^{-12} \cdot \exp(-250/T)$	Burkholder et al. (2015)
$HOCl + OH$	$\rightarrow ClO + H_2O$	$3.00 \times 10^{-12} \cdot \exp(-500/T)$	Burkholder et al. (2015)
$OClO + OH$	$\rightarrow HOCl + O_2$	$1.40 \times 10^{-12} \cdot \exp(600/T)$	Burkholder et al. (2015)
$\mathbf{CFCl_3 + OH}$	$\rightarrow \mathbf{2 \cdot Cl + ClO}$	$1.00 \times 10^{-11} \cdot \exp(-9700/T)$	Burkholder et al. (2015)
$\mathbf{CF_2Cl_2 + OH}$	$\rightarrow \mathbf{Cl + ClO}$	$1.00 \times 10^{-11} \cdot \exp(-11\,900/T)$	Burkholder et al. (2015)
$\mathbf{CH_3Cl + OH}$	$\rightarrow \mathbf{Cl + H_2O}$	$1.96 \times 10^{-12} \cdot \exp(-1200/T)$	Burkholder et al. (2015)
$\mathbf{CH_3Cl + O(^1D)}$	$\rightarrow \mathbf{ClO}$	2.34×10^{-10}	Burkholder et al. (2015)
$\mathbf{CF_2ClBr + OH}$	$\rightarrow \mathbf{Cl + BrO}$	$1.00 \times 10^{-12} \cdot \exp(-3500/T)$	Burkholder et al. (2015)
$\mathbf{CF_2ClBr + O(^1D)}$	$\rightarrow \mathbf{Cl + BrO}$	9.75×10^{-11}	Burkholder et al. (2015)
$\mathbf{CCl_4 + OH}$	$\rightarrow \mathbf{3 \cdot Cl + ClO}$	$1.00 \times 10^{-11} \cdot \exp(-6200/T)$	Burkholder et al. (2015)
$\mathbf{CCl_4 + O(^1D)}$	$\rightarrow \mathbf{3 \cdot Cl + ClO}$	2.61×10^{-10}	Burkholder et al. (2015)
$\mathbf{CF_2ClCFCl_2 + O(^1D)}$	$\rightarrow \mathbf{2 \cdot Cl + ClO}$	2.09×10^{-10}	Burkholder et al. (2015)
$\mathbf{CF_2ClCFCl_2 + OH}$	$\rightarrow \mathbf{2 \cdot Cl + ClO}$	2.32×10^{-10}	Burkholder et al. (2015)
$\mathbf{CHF_2Cl + OH}$	$\rightarrow \mathbf{Cl + H_2O}$	$9.20 \times 10^{-13} \cdot \exp(-1560/T)$	Burkholder et al. (2015)
$\mathbf{CHF_2Cl + O(^1D)}$	$\rightarrow \mathbf{ClO}$	7.65×10^{-11}	Burkholder et al. (2015)
$\mathbf{CH_3CCl_3 + OH}$	$\rightarrow \mathbf{COCl_2 + Cl + H_2O}$	$1.64 \times 10^{-12} \cdot \exp(-1520/T)$	Burkholder et al. (2015)
$\mathbf{CH_3CCl_3 + O(^1D)}$	$\rightarrow \mathbf{2 \cdot Cl + ClO}$	2.93×10^{-10}	Burkholder et al. (2015)
$\mathbf{CF_3Br + OH}$	$\rightarrow \mathbf{Br}$	$1.00 \times 10^{-12} \cdot \exp(-3600/T)$	Burkholder et al. (2015)
$\mathbf{CF_3Br + O(^1D)}$	$\rightarrow \mathbf{BrO}$	4.50×10^{-11}	Burkholder et al. (2015)
$\mathbf{CH_2Br_2 + OH}$	$\rightarrow \mathbf{2 \cdot Br + H_2O}$	$2.00 \times 10^{-12} \cdot \exp(\text{-}840/\text{T})$	Burkholder et al. (2015)
$\mathbf{CH_2Br_2 + O(^1D)}$	$\rightarrow \mathbf{2 \cdot Br + OH}$	2.57×10^{-10}	Burkholder et al. (2015)
$\mathbf{CH_2Br_2 + Cl}$	$\rightarrow \mathbf{2 \cdot Br + HCl}$	$6.30 \times 10^{-12} \cdot \exp(-800/T)$	Burkholder et al. (2015)

Table 3. Continued.

Reactants	Products	Rate constant	Source
$CHBr_3 + OH$	$\rightarrow 3 \cdot Br + H_2O$	$9.00 \times 10^{-13} \cdot \exp(-360/T)$	Burkholder et al. (2015)
$CHBr_3 + O(^1D)$	$\rightarrow 3 \cdot Br + OH$	4.62×10^{-10}	Burkholder et al. (2015)
$CHBr_3 + Cl$	$\rightarrow 3 \cdot Br + HCl$	$4.85 \times 10^{-12} \cdot \exp(-850/T)$	Burkholder et al. (2015)
$CH_2BrCl + OH$	$\rightarrow Br + Cl + H_2O$	$2.10 \times 10^{-12} \cdot \exp(-880/T)$	Burkholder et al. (2015)
$CH_2BrCl + Cl$	$\rightarrow Br + Cl + HCl$	$6.80 \times 10^{-12} \cdot \exp(-870/T)$	Burkholder et al. (2015)
$CHBr_2Cl + OH$	$\rightarrow 2 \cdot Br + Cl + H_2O$	$9.00 \times 10^{-13} \cdot \exp(-420/T)$	Burkholder et al. (2015)
$CHBrCl_2 + OH$	$\rightarrow Br + 2 \cdot Cl + H_2O$	$9.40 \times 10^{-13} \cdot \exp(-510/T)$	Burkholder et al. (2015)
$CF_2ClCF_2Cl + O(^1D)$	$\rightarrow ClO + Cl$	$1.17 \times 10^{-10} \cdot \exp(25/T)$	Burkholder et al. (2015)
$CF_2ClCF_3 + O(^1D)$	$\rightarrow ClO$	$4.64 \times 10^{-11} \cdot \exp(30/T)$	Burkholder et al. (2015)
$CH_3CFCl_2 + O(^1D)$	$\rightarrow ClO + Cl$	1.79×10^{-10}	Burkholder et al. (2015)
$CH_3CF_2Cl + O(^1D)$	$\rightarrow ClO$	1.30×10^{-10}	Burkholder et al. (2015)
$CF_2ClCF_2Cl + OH$	$\rightarrow ClO + Cl$	$1.00 \times 10^{-11} \cdot \exp(-6200/T)$	Burkholder et al. (2015)
$CF_2ClCF_3 + OH$	$\rightarrow ClO$	$1.00 \times 10^{-11} \cdot \exp(-6200/T)$	Burkholder et al. (2015)
$CH_3CFCl_2 + OH$	$\rightarrow 2 \cdot Cl + H_2O$	$1.25 \times 10^{-12} \cdot \exp(-1600/T)$	Burkholder et al. (2015)
$CH_3CF_2Cl + OH$	$\rightarrow Cl + H_2O$	$1.30 \times 10^{-12} \cdot \exp(-1170/T)$	Burkholder et al. (2015)
$CH_2Cl_2 + OH$	$\rightarrow CHCl_2O_2 + H_2O$	$1.92 \times 10^{-12} \cdot \exp(-880/T)$	Burkholder et al. (2015)
$CHCl_3 + OH$	$\rightarrow COCl_2 + Cl + H_2O$	$2.20 \times 10^{-12} \cdot \exp(-920/T)$	Burkholder et al. (2015)
$C_2H_4Cl_2 + OH$	$\rightarrow 2 \cdot Cl + H_2O$	$1.14 \times 10^{-11} \cdot \exp(-1150/T)$	Burkholder et al. (2015)
$CH_2Cl_2 + Cl$	$\rightarrow CHCl_2O_2 + HCl$	$7.40 \times 10^{-12} \cdot \exp(-910/T)$	Burkholder et al. (2015)
$CHCl_3 + Cl$	$\rightarrow COCl_2 + Cl + HCl$	$3.30 \times 10^{-12} \cdot \exp(-990/T)$	Burkholder et al. (2015)
$C_2H_4Cl_2 + Cl$	$\rightarrow 2 \cdot Cl + HCl$	1.30×10^{-12}	Wallington et al. (1996)
$C_2Cl_4 + OH$	$\rightarrow 0.47 \cdot COCl_2 + 3.06 \cdot Cl$	$4.70 \times 10^{-12} \cdot \exp(-990/T)$	Burkholder et al. (2015)
$CHCl_2O_2 + NO$	$\rightarrow 2 \cdot Cl + NO_2 + CO + HO_2$	$4.05 \times 10^{-12} \cdot \exp(360/T)$	MCM3.1
$CHCl_2O_2 + NO_3$	$\rightarrow 2 \cdot Cl + NO_2 + CO + HO_2$	2.30×10^{-12}	MCM3.1
$CHCl_2O_2 + HO_2$	$\rightarrow COCl_2 + H_2O$ $\rightarrow HO_2 + CO + Cl + HOCl$	$3.92 \times 10^{-13} \cdot \exp(700/T)$ $1.68 \times 10^{-13} \cdot \exp(700/T)$	MCM3.1
$CHCl_2O_2 + CH_3O_2$	$\rightarrow 2 \cdot Cl + 2 \cdot HO_2 + CO + HCHO$ $\rightarrow COCl_2 + HCHO + HO_2$	1.20×10^{-12} 0.80×10^{-12}	MCM3.1
$Br_2 + OH$	$\rightarrow Br + HOBr$	$2.10 \times 10^{-11} \cdot \exp(240/T)$	Burkholder et al. (2015)
$Cl_2 + OH$	$\rightarrow Cl + HOCl$	$2.60 \times 10^{-12} \cdot \exp(-1100/T)$	Burkholder et al. (2015)
$HBr + OH$	$\rightarrow Br + H_2O$	$5.50 \times 10^{-12} \cdot \exp(200/T)$	Burkholder et al. (2015)
$ClNO_2 + OH$	$\rightarrow HOCl + NO_2$	$2.40 \times 10^{-12} \cdot \exp(-1250/T)$	Burkholder et al. (2015)
$COCl_2 + O(^1D)$	$\rightarrow CO + ClO + Cl$	$1.76 \times 10^{-10} \cdot \exp(30/T)$	Burkholder et al. (2015)
$Cl_2 + O(^1D)$	$\rightarrow Cl + ClO$	2.03×10^{-10}	Burkholder et al. (2015)

Table 4. Summary of photolysis reactions of atmospheric halogens included in DEST. Reactions absent in the standard StratTrop scheme are highlighted in bold.

Reactant	Products
BrCl	$\rightarrow$ Br + Cl
BrO	$\rightarrow$ Br + (O^3P)
$BrONO_2$	$\rightarrow$ Br + NO_3 $\rightarrow$ Br O + NO_2
OClO	$\rightarrow$ O(^{3}P) + ClO
HOBr	$\rightarrow$ OH + Br
$ClONO_2$	$\rightarrow$ Cl + NO_3 $\rightarrow$ ClO + NO_2
HCl	$\rightarrow$ H + Cl
HOCl	$\rightarrow$ OH + Cl
Cl_2O_2	$\rightarrow 2 \cdot$ Cl + O_2
$CFCl_3$	$\rightarrow 3 \cdot$ Cl
CF_2Cl_2	$\rightarrow 2 \cdot$ Cl
CH_3Br	$\rightarrow$ Br + H
CH_3Cl	**$\rightarrow$ Cl + H**
CF_2ClBr	**$\rightarrow$ Cl + Br**
CCl_4	**$\rightarrow$ $COCl_2$ $+2 \cdot$ Cl**
$CF_2ClCFCl_2$	**$\rightarrow 3 \cdot$ Cl**
CHF_2Cl	**$\rightarrow$ Cl**
CH_3CCl_3	**$\rightarrow 3 \cdot$ Cl**
CF_3Br	**$\rightarrow$ Br**
CH_2Br_2	**$\rightarrow 2 \cdot$ Br**
$CHBr_3$	**$\rightarrow 3 \cdot$ Br**
CF_2ClCF_2Cl	**$\rightarrow 2 \cdot$ Cl**
CF_2ClCF_3	**$\rightarrow$ Cl**
CH_3CFCl_2	**$\rightarrow 2 \cdot$ Cl**
CH_3CF_2Cl	**$\rightarrow$ Cl**
CH_2Cl_2	**$\rightarrow 2 \cdot$ Cl**
$CHCl_3$	**$\rightarrow 3 \cdot$ Cl**
$C_2H_4Cl_2$	**$\rightarrow 2 \cdot$ Cl**
C_2Cl_4	**$\rightarrow 4 \cdot$ Cl**
$COCl_2$	**$\rightarrow 2 \cdot$ Cl + CO**
$ClNO_2$	**$\rightarrow$ Cl + NO_2**
$CHCl_2O_2$	**$\rightarrow$ Cl + ClO + OH**
CH_2BrCl	**$\rightarrow$ Br + Cl**
$CHBr_2Cl$	**$\rightarrow 2 \cdot$ Br + Cl**
$CHBrCl_2$	**$\rightarrow$ Br $+2 \cdot$ Cl**
Cl_2	**$\rightarrow 2 \cdot$ Cl**
Br_2	**$\rightarrow 2 \cdot$ Br**

Regarding photolysis, rather than incorporating the Fast-JX absorption cross sections used in the older CheS+ scheme (Bednarz et al., 2016), DEST includes updated Fast-JX photolysis cross sections for CFC-11, CFC-12, CFC-113, CH_3Cl_3, HCFC-22, Halon-1211, and Halon-1301, using the Stratosphere–troposphere Processes And their Role in Climate (SPARC, 2013) parameterisations to avoid problems with the temperature dependence of the cross sections when calculated using the JPL (2015) recommendations (see SPARC, 2013, for details). Regarding the photolysis lookup tables, which are used in the model instead of Fast-JX at the altitudes above 0.2 hPa, the absorption cross sections for all species were updated following the TOMCAT model (Chipperfield, 1999), with temperature dependence of some of the longer-lived ODSs being further modified, following SPARC (2013).

Finally, the default DEST scheme includes the extended treatment of heterogenous halogen reactions, following Dennison et al. (2019). As detailed in Table 6, in addition to the five standard heterogenous chlorine reactions occurring in StratTrop on nitric acid trihydrate (NAT) PSCs, ice PSCs, and sulfate aerosols, the new DEST scheme includes the $ClONO_2 + HCl$ reaction on sulfate aerosols, eight new heterogeneous bromine reactions, and updated uptake coefficients for the heterogeneous chlorine reactions. We note that while these improvements are now available (but optional) in newer UM–UKCA/UKESM1 versions (vn11.3 and later), these were not yet available in the vn11.0 StratTrop version discussed in this paper (Archibald et al., 2020).

4 DEST evaluation

4.1 Description of the simulations

The performance of our DEST chemistry scheme was evaluated using a 20-year-long (plus spin-up) "time slice" UM–UKCA simulation under perpetual year 2000 conditions. These were created by averaging the forcing data provided for the CMIP6 project (Sellar et al., 2020) over the years 1995–2004 (inclusive). These include greenhouse gas and long-lived ODS data from Meinshausen et al. (2017), sea surface temperatures and sea ice from Durack and Taylor (2016), and emissions of aerosols and chemical tracers of importance in the troposphere, as in Archibald et al. (2020) and Sellar et al. (2020).

Lower boundary conditions for Cl-VSLS are representative of the year 2000 and created by averaging surface station data available in the five latitude bands, namely 90–30° S, 30°–0° S, 0°–30° N, 30–60° N, and 60–90° N. Following Hossaini et al. (2019), NOAA global monitoring network data were used for CH_2Cl_2 and C_2Cl_4 and AGAGE network data were used for $CHCl_3$. The latitude-dependent LBCs for $C_2H_4Cl_2$ were estimated (Hossaini et al., 2016a), based on measurements made during the 2009–2011 HIPPO

Table 5. Summary of the termolecular reactions of the atmospheric halogens included in DEST. Reactions absent in the standard StratTrop scheme are highlighted in bold.

Reactants	Products	Source
$BrO + NO_2 + M$	$\rightarrow BrONO_2 + M$	Sander et al. (2011)[a]
$ClO + ClO + M$	$\rightarrow Cl_2O_2 + M$	Sander et al. (2011)
$Cl_2O_2 + M$	$\rightarrow ClO + ClO + M$	Atkinson et al. (2007)[b]
$ClO + NO_2 + M$	$\rightarrow ClONO_2 + M$	Sander et al. (2011)[c]
$\mathbf{Cl + C_2Cl_4 + M}$	$\mathbf{\rightarrow 5 \cdot Cl + M}$	Burkholder et al. (2015)
$\mathbf{Cl + NO_2 + M}$	$\mathbf{\rightarrow ClNO_2 + M}$	Burkholder et al. (2015)

[a] Sander et al. (2011) data for the low-pressure limit but with 6.9×10^{-12} used for the high-pressure limit. [b] Atkinson et al. (2007) data for the low-pressure limit, with $1.8 \times 10^{14} \exp(-7690/T)$ used for the high-pressure limit. [c] Sander et al. (2011) data for the low-pressure limit but with 1.5×10^{-11} used for the high-pressure limit.

Table 6. Summary of the heterogeneous reactions of the halogen species in DEST. Columns 3–5 indicate the different reaction surfaces (NAT PSCs, ice PSCs, and sulfate aerosols, respectively), and the × symbol indicates that a reaction occurs on a given surface in the model. Different product species to those in the standard StratTrop scheme and/or new reaction surfaces are highlighted in bold. See Dennison et al. (2019) for the corresponding uptake coefficients.

Reactants	Products	NAT	Ice	Aerosols
$ClONO_2 + H_2O$	$\rightarrow HOCl + HONO_2$	×	×	×
$ClONO_2 + HCl$	$\rightarrow \mathbf{Cl_2} + HONO_2$	×	×	**×**
$HOCl + HCl$	$\rightarrow \mathbf{Cl_2} + H_2O$	×	×	×
$N_2O_5 + H_2O$	$\rightarrow \quad 2 \cdot HONO_2$	×	×	×
$N_2O_5 + HCl$	$\rightarrow \mathbf{ClNO_2} + HONO_2$	×	×	
$ClONO_2 + HBr$	$\rightarrow BrCl + HONO_2$	**×**	**×**	
$HOCl + HBr$	$\rightarrow BrCl + H_2O$		**×**	
$HOBr + HCl$	$\rightarrow BrCl + H_2O$		**×**	
$BrONO_2 + HCl$	$\rightarrow BrCl + HONO_2$		**×**	**×**
$BrONO_2 + H_2O$	$\rightarrow HOBr + HONO_2$		**×**	**×**
$HOBr + HBr$	$\rightarrow \mathbf{Br_2} + H_2O$		**×**	
$BrONO_2 + HBr$	$\rightarrow \mathbf{Br_2} + HONO_2$		**×**	
$N_2O_5 + HBr$	$\rightarrow Br + NO_2 + HONO_2$	**×**		

aircraft campaign (Wofsy, 2011). The Br-VSLS emissions are also climatological and follow Ordóñez et al. (2012). As a benchmark for comparison with DEST, a second 20-year-long (plus spin-up) simulation was performed under the same time slice year 2000 conditions but using the standard StratTrop scheme described and evaluated in Archibald et al. (2020).

In addition to the above time slice simulations, a set of analogous transient (2000–2019) experiments was performed using the new DEST scheme with time-varying Cl-VSLS LBCs. This consisted of a three-member ensemble of free-running simulations and a simulation in which the meteorology was nudged towards the ERA5 reanalysis (Hersbach et al., 2020). These transient runs are described in detail in Bednarz et al. (2022; where they are referred to as "VSLS" and "$VSLS_{SD-5}$", respectively) and are used here for a comparison of the model results with observational and reanalysis datasets.

We note two problems in the code present in the time slice year 2000 DEST simulations discussed in Sect. 4.2; note that these are fixed in the final DEST (vn1.0) version lodged in UM–UKCA (vn11.0) and in the transient DEST simulations used here in Sect. 4.3 and in Bednarz et al. (2022). First, the bimolecular reaction of $COCl_2$ with $O(^1D)$ produces one molecule of CO and ClO each, instead of one molecule of CO, ClO, and Cl; this results in a loss of one chlorine atom per reaction. Second, the update to the photolysis cross section of CFC-113 after SPARC (2013) discussed in Sect. 3.4 was not included, so the reaction proceeds with the old absorption cross section used in CheS+ scheme in Bednarz et al. (2016). As shown in Fig. S1a in the Supplement, the cumulative effect of the two issues under the mean 2010–2019 conditions is to underestimate the total chlorine levels by $\sim$ 1–2 ppt in the stratosphere; this constitutes a very small fraction of the total stratospheric chlorine content ($\sim$ 3.3–3.4 ppb). In the absence of Cl-VSLS, on the other hand, the cumulative effect changes sign, leading in turn to a similarly small overestimation of the stratospheric chlorine levels by $\sim$ 1–2 ppt (Fig. S1b). While we acknowledge that both issues are important, especially for studies focusing on Cl-VSLS, and have been fixed in the final DEST vn1.0 version that is now lodged in vn11.0 of UM–UKCA and used for science studies (e.g. Bednarz et al., 2022), the two effects should thus not have a dominant impact on the time slice year 2000 evaluation results in Sect. 4.2.

4.2 Comparison between DEST and StratTrop

4.2.1 Stratospheric and tropospheric halogens

Figure 1 shows yearly mean differences in total chlorine and bromine volume mixing ratios (i.e. including contributions from both source and product gases) between our new DEST scheme and the standard StratTrop scheme. We find that DEST shows 40–60 ppt more chlorine in the lower stratosphere, with larger differences of up to $\sim$ 150 ppt simulated

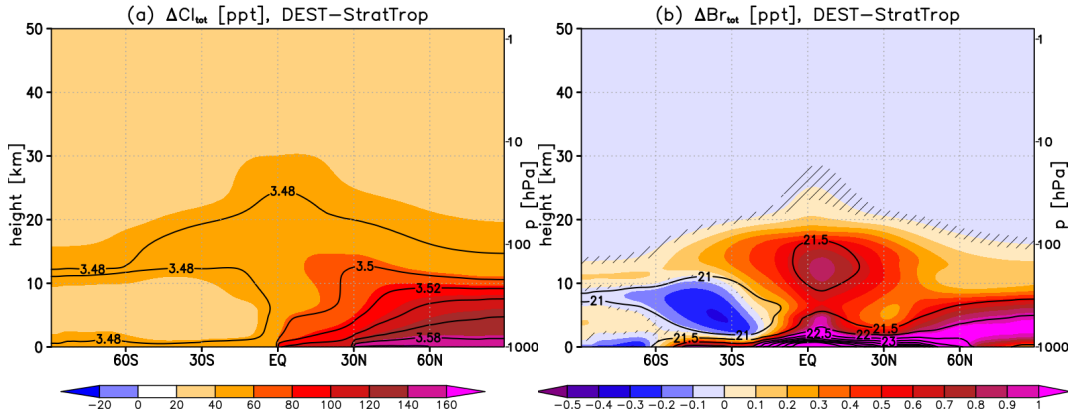

Figure 1. The shading indicates the annual mean difference (ppt) in simulated total Cl **(a)** and total Br **(b)** between DEST and StratTrop for the year 2000 conditions. The hatching denotes regions where the difference is not statistically significant, which is here taken as being lower than ±2 standard errors. Contours show the corresponding values in DEST for reference; note that in panel **(a)**, this is plotted in units of parts per billion.

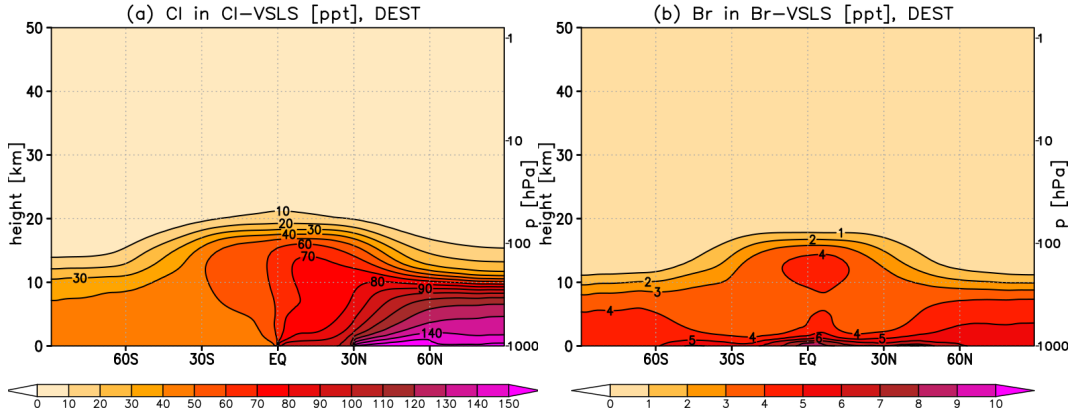

Figure 2. Annual mean Cl in Cl-VSLS **(a)** and Br in Br-VSLS **(b)** (ppt) simulated in DEST for the year 2000 conditions.

in the Northern Hemisphere (NH) troposphere. These differences arise largely from the inclusion of Cl-VSLS in the model, with Cl-VSLS source gases accounting for most of the additional chlorine near the surface (Fig. 2a). In comparison, the associated difference in near-surface total chlorine found in the form of long-lived ODSs is only 4 ppt (with lower values in DEST than in StratTrop; cf. 3.4 ppb total near-surface chlorine in ODSs).

For bromine, we find no substantial differences in the total stratospheric bromine content between DEST and StratTrop over large parts of the stratosphere (Fig. 1b). In the lowermost stratosphere, however, DEST simulates higher bromine levels compared to StratTrop (e.g. by 0.3 ppt in the tropics, 25° N–25° S, at 18 km or by 0.2 ppt at 51° N and 15 km). Total bromine levels are also markedly higher in DEST in the tropical and NH troposphere (e.g. up to ∼ 0.8 ppt more bromine in the equatorial upper troposphere). These increases arise from the inclusion of Br-VSLS in DEST, the elevated levels of which are simulated throughout the troposphere and lowermost stratosphere (Fig. 2b). We calculate the resulting Br-VSLS stratospheric source gas injection in DEST to be 1.9 ppt Br (at 17 km, 20° N–20° S, for the time slice year 2000 conditions), which is in a good agreement with the intermodel mean value of 1.5–2.5 ppt, as derived in Hossaini et al. (2016b). We note that in the Southern Hemisphere (SH) troposphere, on the other hand, DEST shows somewhat lower bromine levels compared to StratTrop (up to ∼ −0.3 ppt in the midlatitudes). This may be related to the somewhat smaller near-surface bromine levels simulated in the SH high latitudes and/or differences in the lifetime of the species that bromine is present in (as discussed in Sect. 3.2; while the standard StratTrop scheme does not include an explicit representation of Br-VSLS, their contribution to the total bromine budget is approximated by adding an extra 5 ppt bromine to the LBCs of CH_3Br).

Regarding long-lived ODSs, DEST shows smaller levels of halogens present in the form of ODS source gases in the lower stratosphere compared to StratTrop and higher levels in the mid- and upper stratosphere (Fig. 3). For bromine, we also find a 4–5 ppt reduction in bromine in long-lived

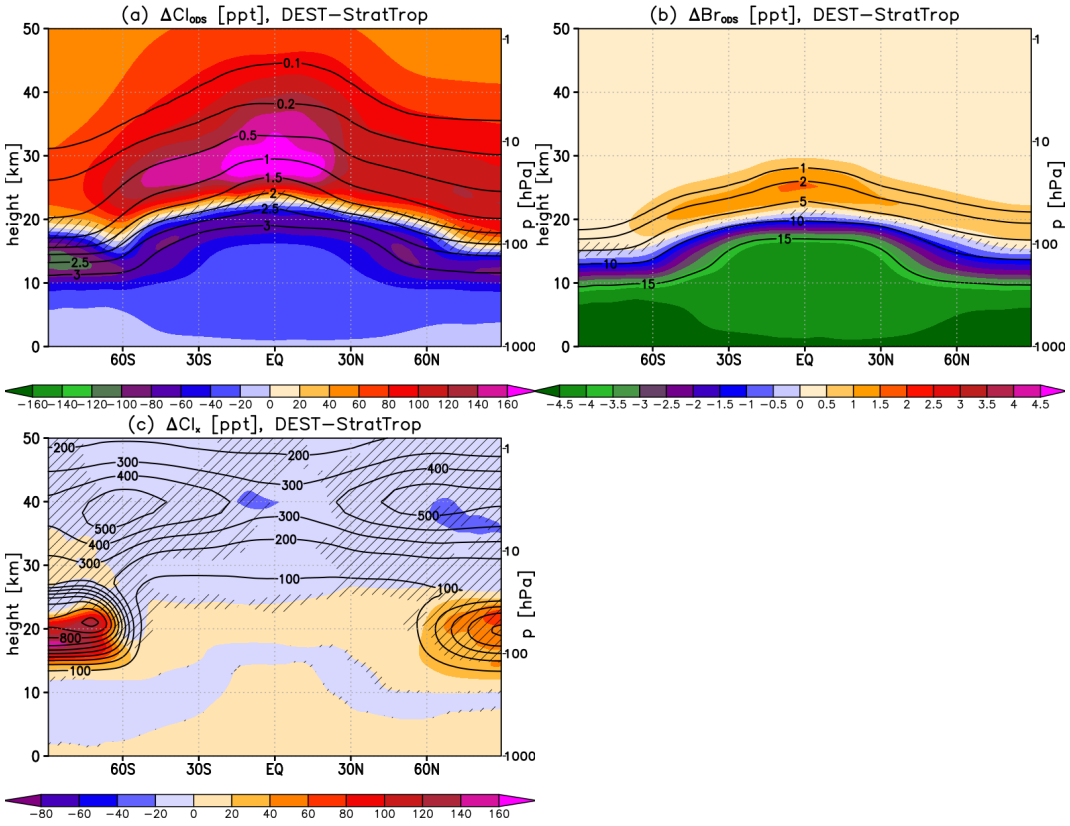

Figure 3. The shading indicates the annual mean difference (ppt) in Cl present in long-lived ODSs, Cl_{ODS} **(a)**, Br present in long-lived ODSs, Br_{ODS} **(b)**, and total reactive chlorine, Cl_x (with $Cl_x = ClO + 2 \cdot Cl_2O_2 + Cl + OClO + 2 \cdot Cl_2$), between DEST and StratTrop for the year 2000 conditions. The hatching denotes regions where the difference is not statistically significant, which is taken here as being lower than ± 2 standard errors. Contours show the corresponding values in DEST for reference; note that in panel **(a)**, this is plotted in units of parts per billion.

ODSs in the troposphere (Fig. 3b; with a 4.9 ppt reduction in bromine in ODSs near the surface); this is in accord with the 5 ppt bromine included in StratTrop in the LBCs of CH_3Br to account for the bromine contribution from Br-VSLS (Sect. 3.2), which in DEST is instead represented explicitly (Fig. 2b).

Figure 4 shows the associated differences in some of the main inorganic halogen species. The elevated tropospheric and lower-stratospheric chlorine levels in DEST (Fig. 1a) compared to StratTrop increase HCl and $ClONO_2$ – the main chlorine reservoirs – in the lower stratosphere (Fig. 4a and b). Above, in the mid- and upper stratosphere, DEST shows a decrease in HCl and $ClONO_2$, which is in accord with the concurrent higher levels of chlorine present in the form of long-lived ODSs (Fig. 3a).

For bromine, DEST shows an increase in BrO in the tropical tropopause layer (TTL) and upper troposphere and lower stratosphere (UTLS) and a decrease in BrO above (Fig. 4f); this is thus qualitatively similar to what was found for HCl. The BrO increase is related to the higher total bromine levels simulated in the lowermost stratosphere as the result of including Br-VSLS (as discussed above) and the inclusion of heterogenous bromine reactions (Sect. 3.4) that increase the BrO to total inorganic bromine (Br_y) ratio through the conversion of bromine reservoirs (e.g. HBr). Previous box model analysis highlighted a strong sensitivity of the BrO / Br_y ratio in the TTL to the aerosol and ice surface area density (e.g. Koenig et al., 2017). The decrease in BrO directly above arises because of the concurrent increase in bromine levels found in the form of long-lived ODSs at these altitudes (Fig. 3b). For $BrONO_2$, its concentrations are lower in DEST throughout the stratosphere (Fig. 4e) compared to StratTrop, and this is partially related to the concurrent increase in stratospheric concentrations of BrCl (Fig. 4c). Regarding HBr, DEST shows a significant increase in HBr throughout the troposphere as the result of the increase in the total tropospheric bromine from including Br-VSLS, with a decrease in HBr simulated in the stratosphere (Fig. 4d).

Figure 3c also shows the corresponding annual and zonal mean difference in total reactive chlorine (Cl_x, with $Cl_x = ClO + 2 \cdot Cl_2O_2 + Cl + OClO + 2 \cdot Cl_2$) between DEST and StratTrop. We find markedly higher levels of reactive chlorine in DEST in the high-latitude lower stratosphere in both hemispheres (i.e. by up to ~ 140 ppt in the

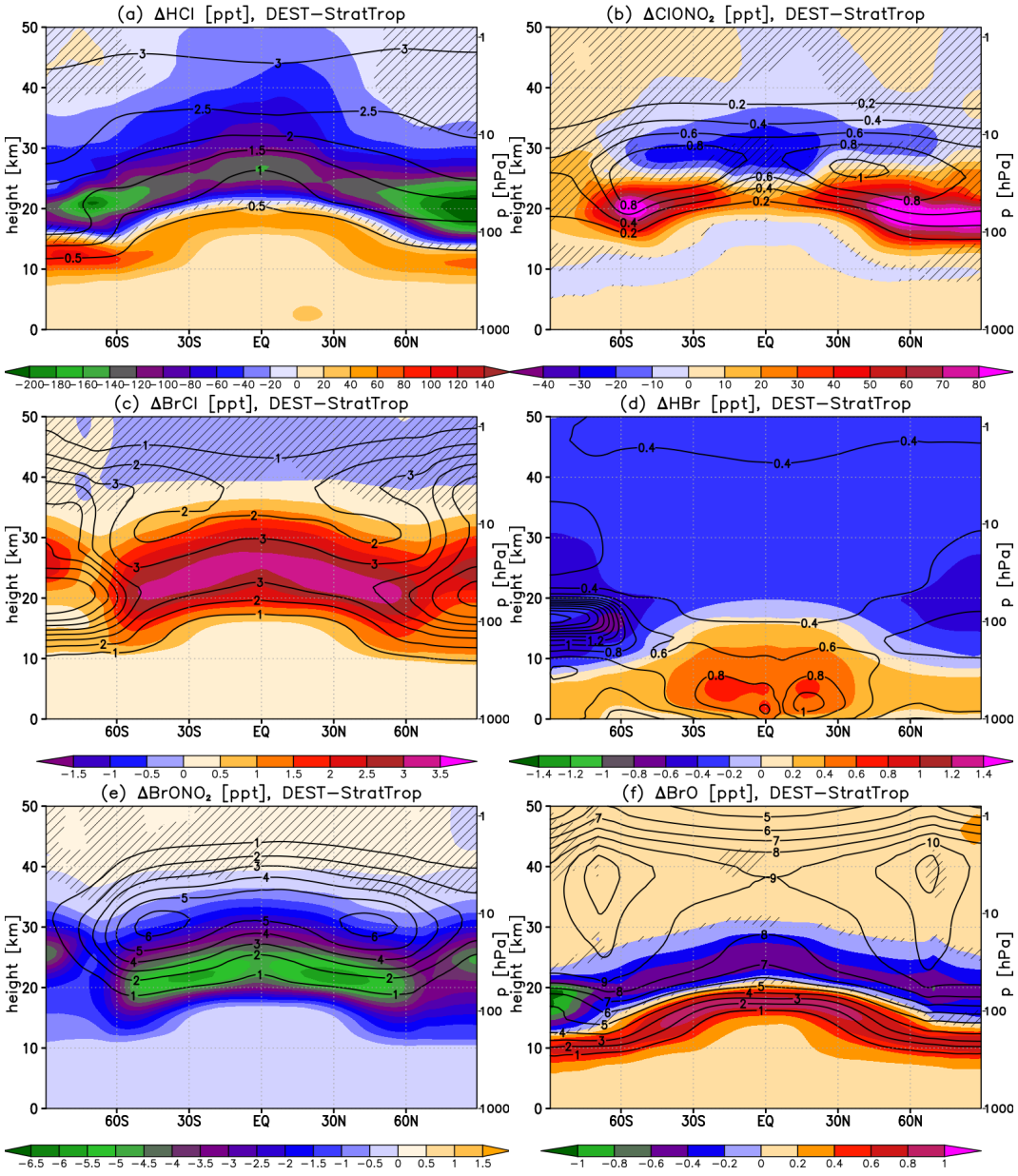

Figure 4. The shading indicates the annual mean difference (ppt) in the simulated HCl **(a)**, $ClONO_2$ **(b)**, BrCl **(c)**, HBr **(d)**, $BrONO_2$ **(e)**, and BrO **(f)** between DEST and StratTrop for the year 2000 conditions. The hatching is the same as in Fig. 1. Contours show the corresponding values in DEST for reference; note that in panels **(a)** and **(b)**, this is plotted in units of parts per billion.

SH and ∼ 60 ppt in the NH in yearly mean). These yearly mean values correspond to accelerated heterogenous reactions on PSCs and aerosols inside the polar vortices in winter and spring. The response reflects the combined impact of the updates to the heterogeneous halogen reactions (Sect. 3.4), as already discussed in Dennison et al. (2019), and the increase in total stratospheric chlorine in DEST compared to StratTrop (Fig. 1a) as the result of including Cl-VSLS.

4.2.2 Stratospheric ozone

The increase in reactive chlorine (Fig. 3c) and bromine (BrO and BrCl; Fig. 4f and c) in the lower stratosphere in DEST has important consequences for stratospheric ozone concentrations simulated in the model (Fig. 5). We find significant reductions in lower-stratospheric ozone levels throughout the globe in DEST compared to StratTrop, with up to ∼ 4 % decrease in the lower-stratospheric ozone simulated in the tropics (Fig. 5a). In the high latitudes during spring, the ozone reduction reaches locally ∼ 75 % in the SH (Fig. 5b)

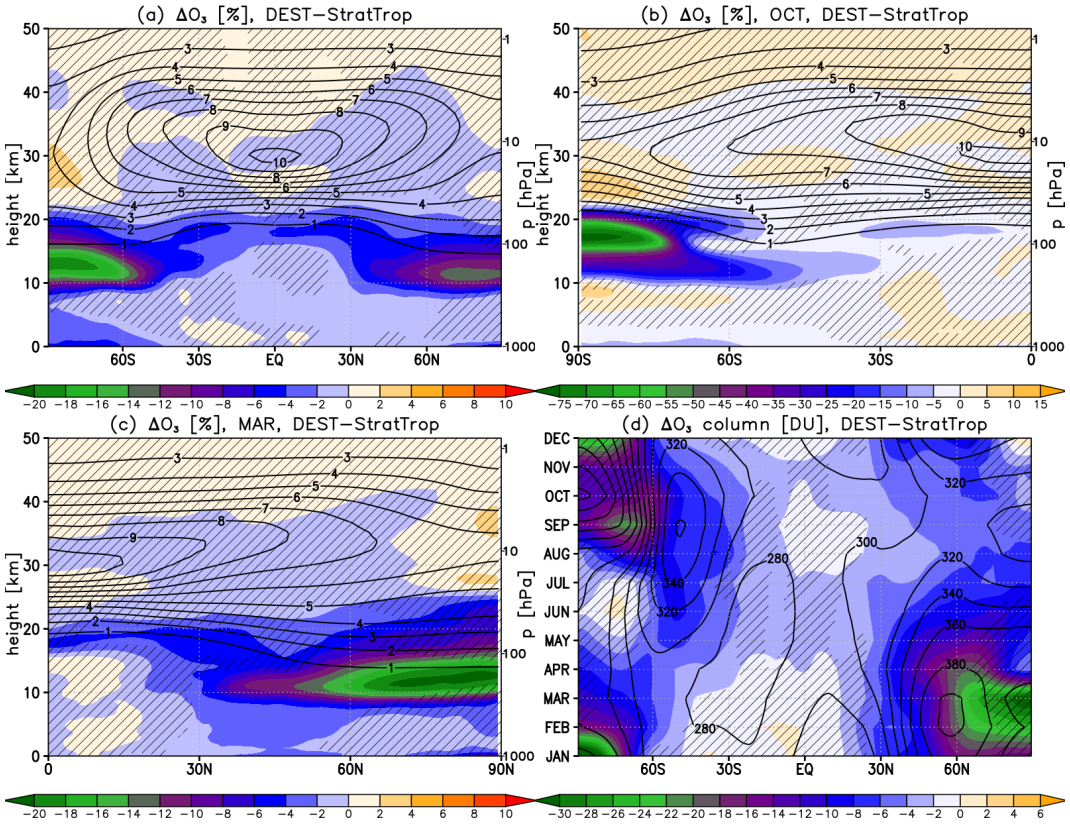

Figure 5. The shading indicates the difference in annual mean O_3 (%) **(a)**, southern hemispheric O_3 (%) in October **(b)**, northern hemispheric O_3 (%) in March **(c)**, and total column O_3 as a function of latitude and month (DU) **(d)** between DEST and StratTrop for the year 2000 conditions. The hatching is the same as in Fig. 1. Contours show the corresponding values in DEST for reference (in units of ppm for panels **a–c** and in units of DU in panel **d**).

and $\sim 20\,\%$ in the NH (Fig. 5c). When integrated over the depth of the atmosphere, statistically significant decreases in total column O_3 are generally found in DEST in the mid-latitudes, with up to 16 and 20 DU lower total column O_3 found at 60° S and 60° N in October and March, respectively (Fig. 5d).

4.2.3 Stratospheric climate

The reduction in stratospheric ozone levels in DEST relative to StratTrop affects stratospheric climate. The decrease in ozone in the tropical lower-stratosphere results in a small but statistically significant cooling of $\sim 0.2\,\mathrm{K}$ in the region (Fig. 6a). The decrease in tropical cold-point temperatures in turn reduces the amount of water vapour entering the stratosphere, resulting in up to $\sim 3\,\%$ higher lower-stratospheric water vapour levels in DEST compared to StratTrop (Fig. 6b). Changes in lower-stratospheric temperatures also impact the large-scale transport, manifested by the slightly younger stratospheric age of air (AoA; Fig. 6c), presumably as the consequence of the reduction in tropical tropospheric static stability and thus enhanced upwelling. The changes in transport further impact the concentrations of halogenated source and product gases (Sect. 4.2.1).

In the SH high latitudes, the DEST simulation also shows a local cooling in the lower stratosphere and a warming above. The response is a signature of an accelerated Antarctic springtime ozone depletion and its impact on the SH polar vortex, as was found in a number of studies in the context of the impact of ODSs on Antarctic ozone (e.g. MacLandress et al., 2011; Keeble et al., 2014).

4.3 Comparison between DEST and observations or reanalysis

We now evaluate the performance of DEST against observations and reanalysis. In order to facilitate better comparison with observational datasets, rather than using the time slice year 2000 simulation discussed in Sect. 4.2., we use the transient 2000–2019 integrations with either free-running or nudged meteorology, as described in Bednarz et al. (2022). In addition to using time-varying forcings, these use the final DEST version, where the two problems in the code present in the time slice year 2000 integrations, discussed in Sect. 4.2, have been fixed (see Sect. 4.1). While the objective of our

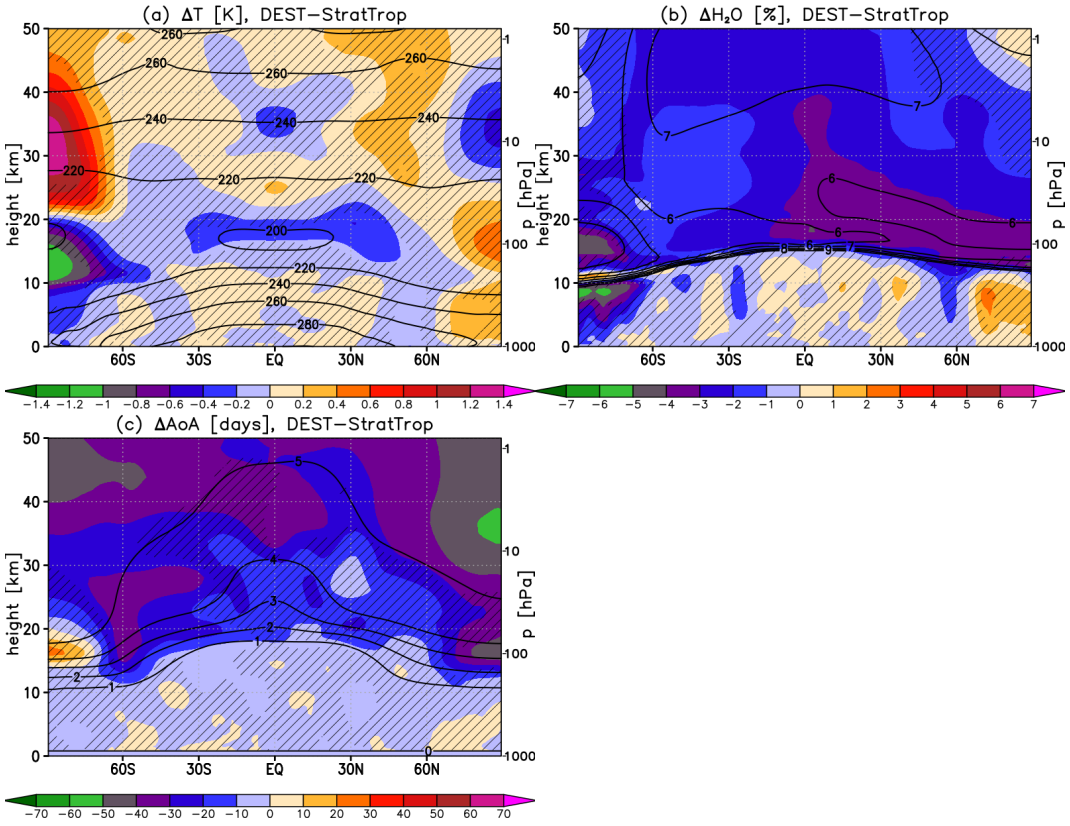

Figure 6. As in Fig. 4 but for the difference in temperature (K) **(a)**, specific humidity (%) **(b)**, and model age of air (d) **(c)**. Note that the contours in panels **(b)** and **(c)** are in the units of parts per million and years, respectively.

previous work was to isolate and analyse the impact of Cl-VSLS on the stratospheric halogen budget, here we focus on evaluating the overall performance of the DEST scheme.

Figures 7 and 8 compare the surface concentrations of $CHBr_3$ and CH_2Br_2 measured over 2010–2018 at a number of NOAA monitoring sites (updated from Hossaini et al., 2016b; see also https://gml.noaa.gov, last access: 29 August 2022) to those simulated in the free-running DEST runs at the same locations. We find that the inclusion of Br-VSLS emissions results in relatively good agreement with observations at most of the sites analysed. Some exceptions remain, however, especially for bromoform, whose simulated concentrations tend to be too small in the NH mid- and high latitudes and too large at some of the sites in the NH subtropics.

Figures 9 and 10 compare the DEST-simulated HCl, ozone, $COCl_2$, and water vapour levels with the Atmospheric Chemistry Experiment Fourier Transform Spectrometer (ACE-FTS vn3.5-3.6) satellite data (Boone et al., 2013). We find that the DEST runs significantly overestimate HCl in the tropical (up to ~ 0.2 ppb) and high-latitude (up to ~ 0.8 ppb over the Antarctic) lower stratosphere compared to ACE-FTS (Figs. 9a and 10a); the Antarctic bias is smaller (up to ~ 0.4 ppb) under the nudged meteorology set-up (Fig. 10a). The simulations also underestimate HCl over the rest of the stratosphere (by up to ~ -0.2–0.3 ppb), compared to ACE-FTS, although in the middle and upper stratosphere this underestimation falls within the range of the ACE-FTS measurement error (Fig. S2a). As shown in Bednarz et al. (2022), the inclusion of Cl-VSLS in the model increases HCl throughout the stratosphere; this effect thus acts to improve the model–measurement comparison in the mid- and upper stratosphere.

For ozone, DEST shows ozone concentrations that are too high in the tropical upper troposphere and lower stratosphere (Figs. 9b and 10b). The reduction in tropical lower-stratospheric ozone in DEST compared to StratTrop (Fig. 5a) implies that DEST performs better in this respect than StratTrop. The opposite is true for the high latitudes, as the transient DEST runs underestimate lower-stratospheric ozone in the polar regions compared to ACE-FTS (Figs. 9b and 10b), and the reduction in polar ozone in DEST compared to StratTrop (Fig. 5a) worsens the comparison with satellite data. We note that the comparison is made only with one satellite dataset, while important uncertainties exist in most observational datasets. For instance, a small positive bias of a few percent in the lower-stratospheric ozone concentrations was

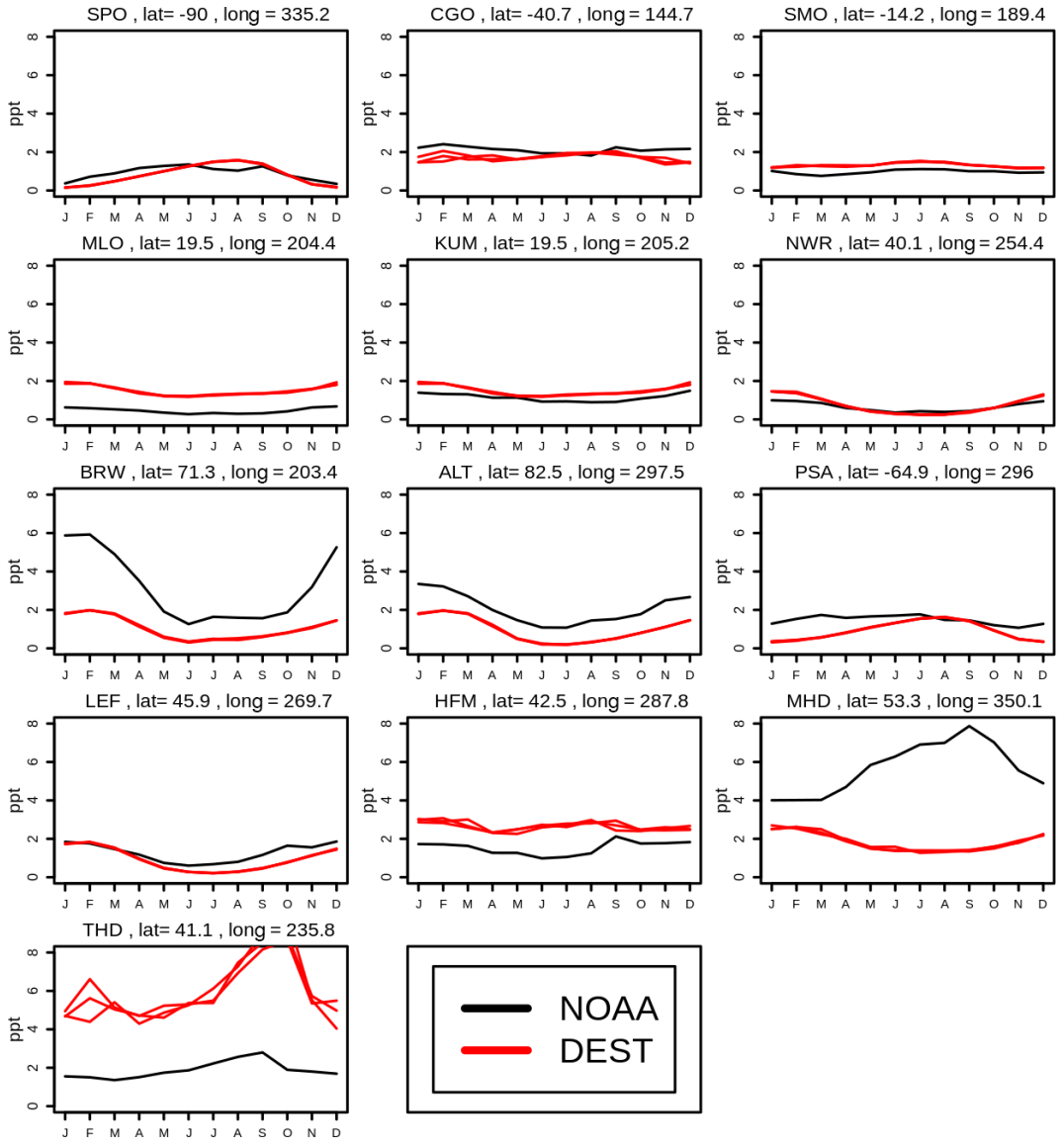

Figure 7. Monthly mean evolution of 2010–2018 climatological surface $CHBr_3$ concentrations (ppt) measured by different NOAA measurement sites (updated from Hossaini et al., 2016b; black) and the corresponding concentrations simulated at these locations in the individual ensemble members of the transient free-running DEST experiment (red). The code names for the different sites are as follows: SPO is for the South Pole, Antarctica; CGO is for Kennaook / Cape Grim, Australia; SMO is for Tutuila, American Samoa; MLO is for Mauna Loa, HI, USA; KUM is for Cape Kumukahi, HI, USA; NWR is for Niwot Ridge, CO, USA; BRW is for Point Barrow, AK, USA; ALT is for Alert, Canada; PSA is for Palmer Station, Antarctica; LEF is for Park Falls, WI, USA; HFM is for Harvard Forest, MA, USA; MHD is for Mace Head, Ireland; and THD is for Trinidad Head, CA, USA. The DEST values at THD reach 8.6–9.9 ppt in October for the individual ensemble members.

reported for vn3.6 of the ACE-FTS data used here (Sheese et al., 2022).

For phosgene, DEST with free-running meteorology compares reasonably well in the tropics at ∼ 20 km altitude but underestimates the phosgene levels in other regions (Fig. 9c); we note the relative uncertainties in the ACE-FTS $COCl_2$ levels are very high (Fig. S2b). When the meteorology is nudged, DEST-simulated $COCl_2$ becomes slightly positively biased in the extratropical lower stratosphere above ∼ 20 km compared to ACE-FTS (Fig. 10c). $COCl_2$ is not included at all in StratTrop, and so it follows that the standard scheme omits this important stratospheric chlorine species.

Regarding stratospheric water vapour, the free-running DEST simulations significantly overestimate stratospheric water vapour compared to ACE-FTS (up to ∼ 2.0–2.5 ppm in the tropical lower stratosphere; Fig. 9d); this likely arises because of markedly warmer tropical lower stratosphere in the model (by ∼ 2 K at 100 hPa compared to ERA-Interim;

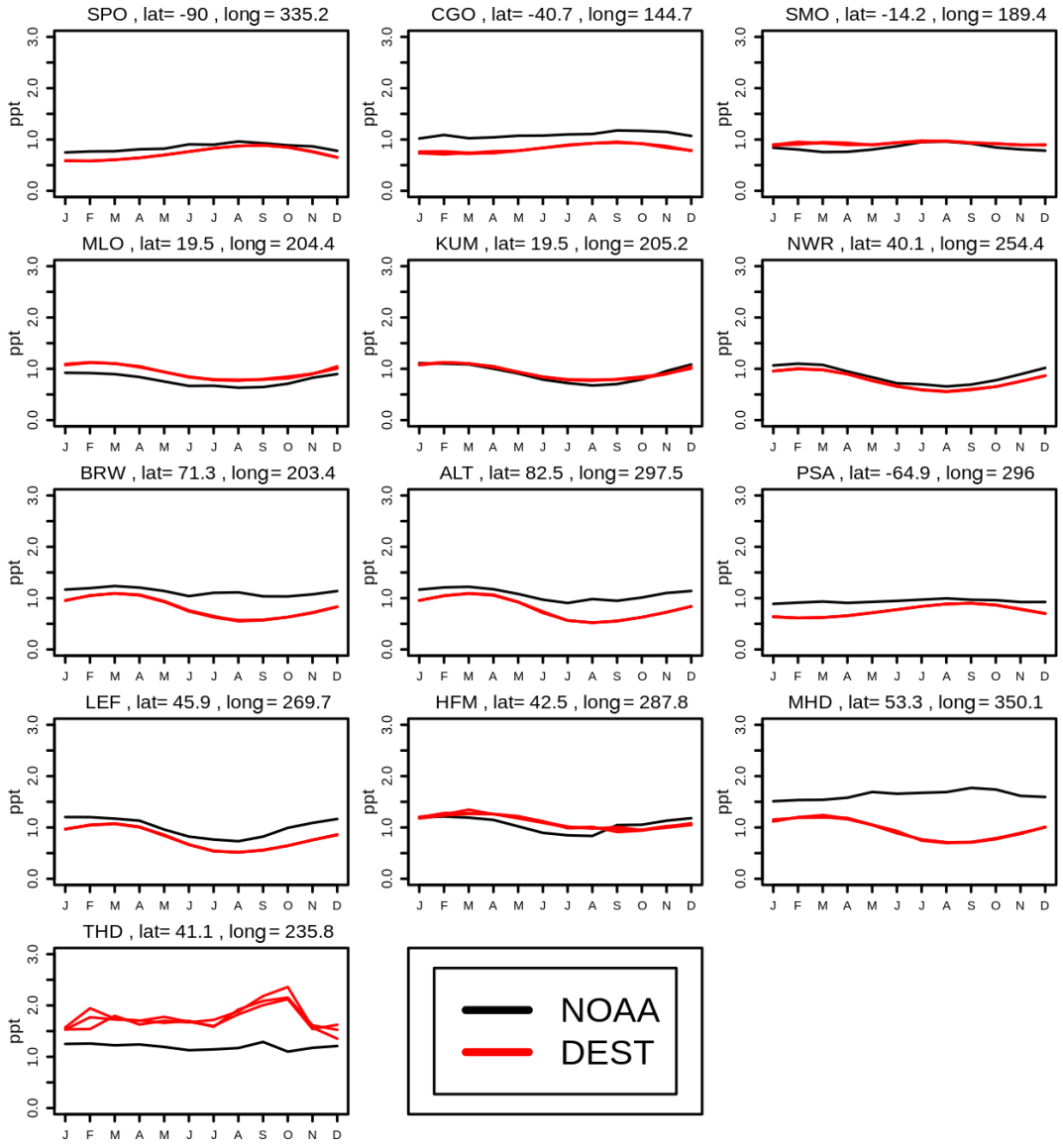

Figure 8. As in Fig. 7 but for CH_2Br_2 (ppt).

Fig. 11a) facilitating too much input of water vapour to the stratosphere. Accordingly, the positive water vapour bias is no longer present in the nudged DEST configuration (Fig. 10d). Since the reduction in tropical lower-stratospheric ozone in DEST compared to StratTrop (Fig. 5a) was shown to reduce tropical cold-point temperatures (Fig. 6a) and thus stratospheric water vapour levels (Fig. 6b), it follows that DEST acts to slightly reduce the positive water vapour bias found in the free-running configuration compared to the standard StratTrop version.

Figure 11 compares the DEST simulated temperatures and zonal winds to the ERA-Interim reanalysis (Dee et al., 2011). In the SH high-latitudes, DEST under free-running meteorology simulates a lower stratosphere that is too cold and a SH polar vortex that is too strong compared to ERA-Interim (Fig. 8); such a bias is common to several chemistry–climate models (e.g. Morgenstern et al., 2022). Since the reduction in Antarctic ozone in DEST compared to StratTrop results in cooling in the Antarctic lower stratosphere (Fig. 6a), it follows that in this respect the comparison with reanalysis is worse for DEST than for the standard StratTrop scheme.

To summarise, we find that the impact of the new DEST developments (compared to StratTrop) improves some aspects of the comparison with satellite observations or reanalysis, although it also worsens other aspects. We note, however, that the simulated concentrations of atmospheric tracers and fields are the cumulative result of a range of chemical, radiative, and dynamical processes, and so an improvement in a small subset of these does not necessarily guarantee a better model agreement with observations or reanalysis.

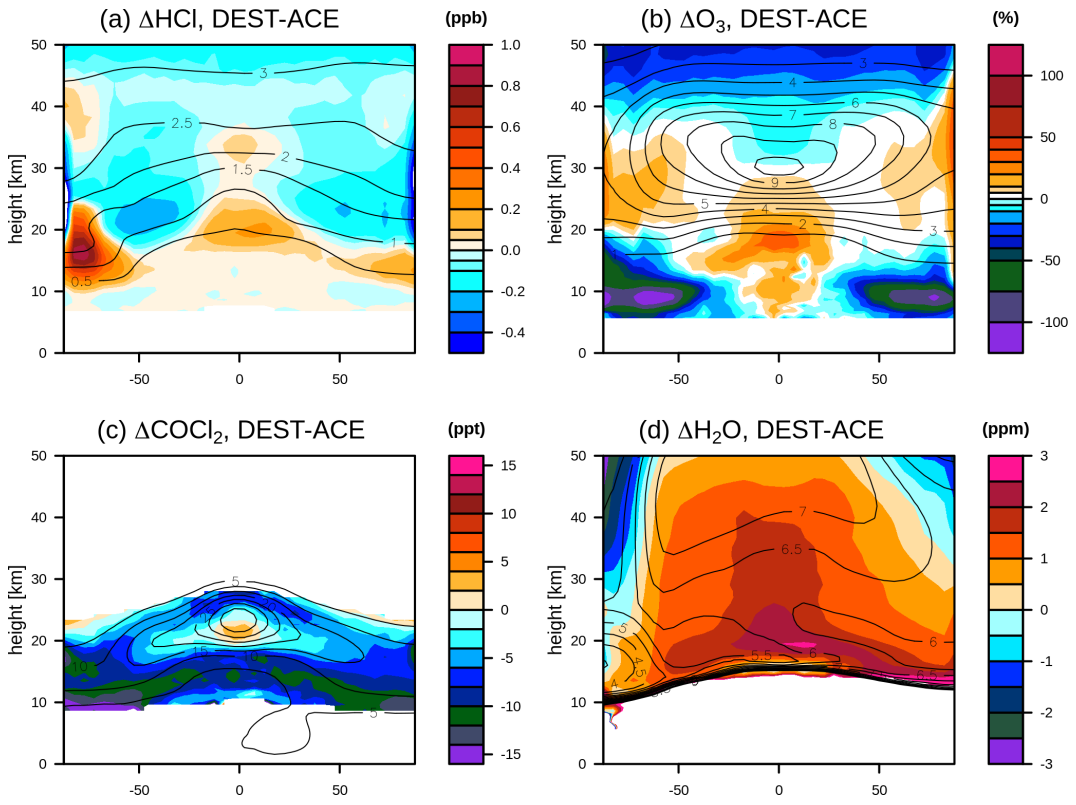

Figure 9. The shading indicates the 2005–2019 annual mean difference in **(a)** HCl (ppb), **(b)** O_3 (%), **(c)** $COCl_2$ (ppt), and **(d)** H_2O (ppm) between the ensemble mean transient free-running DEST simulations and the Atmospheric Chemistry Experiment Fourier Transform Spectrometer (ACE-FTS vn3.5-3.6) data. Contours show the corresponding DEST climatology for reference. See Fig. S2 in the Supplement for the corresponding errors in the ACE-FTS values. The percentage difference in panel **(b)** is calculated relative to the model values.

For dynamical fields in particular (e.g. the Antarctic vortex that is too cold and too strong in the model, as mentioned above), model parameterisations are tuned to reproduce observed climatologies. Thus, a change in a chemistry scheme can result in a degradation of model performance, potentially requiring further tuning (Morgenstern et al., 2022). In addition, the study uses only one satellite dataset (ACE-FTS vn3.5-3.6) and one reanalysis (ERA-Interim), while substantial uncertainties exist in most of the observational and reanalysis datasets, and differences are commonly found between different satellite or reanalysis products (e.g. SPARC/IO3C/GAW, 2019).

5 Summary and outlook

We have described the development and performance of the new Double Extended Stratospheric–Tropospheric (DEST vn1.0) chemistry scheme, which constitutes part of the UM–UKCA chemistry–climate model, the atmospheric composition model of UKESM1 (Sellar et al., 2019). The DEST scheme is an extension of the standard Stratospheric–Tropospheric chemistry scheme (StratTrop; Archibald et al., 2020) that includes a range of important updates to the halogen chemistry, allowing process-oriented studies of stratospheric ozone depletion and recovery, including the impacts from both controlled long-lived ozone-depleting substances and uncontrolled halogenated very-short substances. The main updates in DEST are (i) an explicit treatment of 14 of the most important long-lived ODSs; (ii) an inclusion of Br-VSLS emissions and chemistry; and (iii) an inclusion of Cl-VSLS emissions/LBCs and chemistry. Further updates include the inclusion of additional inorganic halogen tracers and changes to the photolysis, gas phase, and heterogeneous reaction rates (the latter following Dennison et al., 2019). As a result, the DEST scheme improves on some of the important shortcomings in the representation of halogens in the standard StratTrop scheme that is currently being used in the UKESM1 CCMI-2022 simulations in support of the WMO and UNEP Ozone Assessment Reports and, thus, will be particularly relevant for studies informing the future reports.

The performance of DEST was evaluated against the standard StratTrop scheme and against the ACE-FTS satellite observations and the ERA-Interim reanalysis. We found larger lower-stratospheric total chlorine levels ($\sim$ 40–60 ppt Cl for the year 2000 conditions) in DEST compared to StratTrop, as well as significant changes in tropospheric total chlorine and

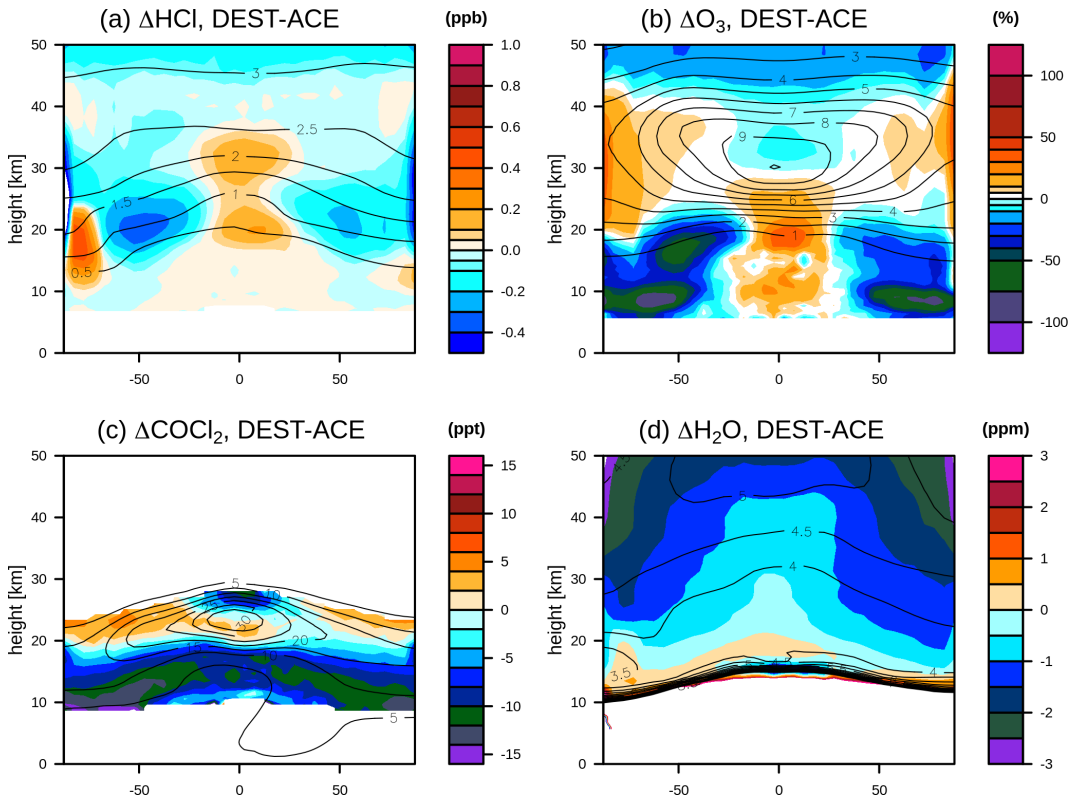

Figure 10. As in Fig. 9 but for the nudged DEST simulation.

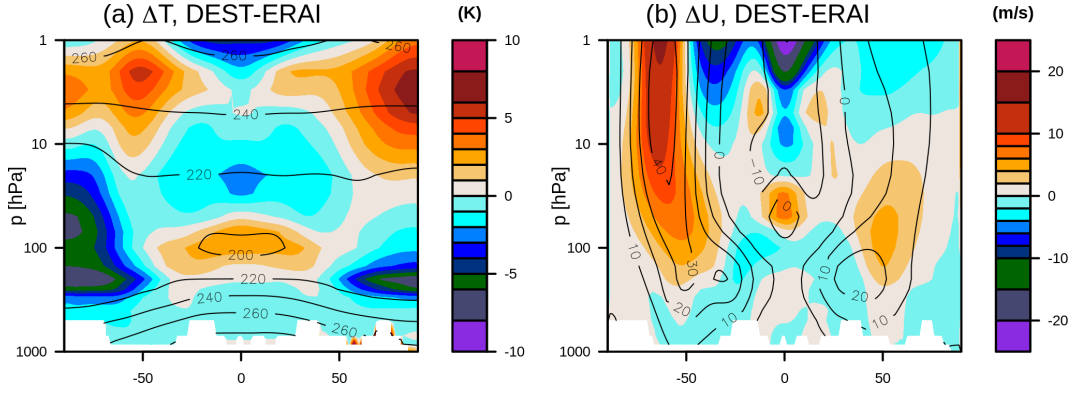

Figure 11. The shading indicates the 2005–2018 annual mean difference in the zonal mean temperature (K) **(a)** and **(b)** zonal wind ($m\,s^{-1}$) between the ensemble mean transient free-running DEST simulations and ERA-Interim reanalysis. Contours show the corresponding DEST climatology for reference.

bromine levels and their horizontal distributions. Total stratospheric bromine levels were found to be similar between the DEST and StratTrop over large parts of the stratosphere, with the exception of the lowermost stratosphere, where DEST showed higher bromine levels (e.g. by 0.3 ppt in the tropics at 18 km altitude). The changes in total halogen levels in the stratosphere were accompanied by marked changes in the speciation of inorganic halogen species and in the levels of halogens found in the form of longer-lived ODSs. The resulting impacts on stratospheric ozone, water vapour, temperature, and transport were also discussed.

Future improvements in DEST vn2.0 will incorporate iodine chemistry, which has now emerged as a potentially important contributor to both processes in the troposphere and to stratospheric ozone depletion (e.g. Koenig et al., 2020; Cuevas et al., 2022).

Code and data availability. The data from all UM–UKCA simulations used in this work and the plotting scripts used to make all figures are available from https://doi.org/10.5281/zenodo.7033255 (Bednarz, 2022). ACE-FTS data can be obtained from http://www.ace.uwaterloo.ca/data.php (Boone et al., 2013). ERA-Interim data can be obtained from https://www.ecmwf.int/en/forecasts/datasets/reanalysis-datasets/era-interim (Dee et al., 2011). The NOAA surface measurements of $CHBr_3$ and CH_2Br_2 (Montzka et al. 2015) will be available from https://gml.noaa.gov/; please contact Steve Montzka (stephen.a.montzka@noaa.gov) if you require access to it.

All simulations used in this work were performed using version 11.0 of the Met Office Unified Model coupled to the United Kingdom Chemistry and Aerosol model (UM–UKCA). The UM and/or JULES (the Joint UK Land Environment Simulator) code branch(es) used in the publication have not all been submitted for review and inclusion in the UM–JULES trunk or released for general use. However, the UM and JULES code branches were made available to reviewers of this paper. Due to intellectual property copyright restrictions, we cannot provide the source code for UM–UKCA. The UM–UKCA model is available for use through a licensing agreement. A number of research organisations and national meteorological services use UM–UKCA in collaboration with the Met Office to undertake basic atmospheric process research, produce forecasts, develop the model code, and build and evaluate Earth system models. Please visit https://www.metoffice.gov.uk/research/approach/modelling-systems/unified-model (last access: 15 July 2022) for further information on how to apply for a licence.

Supplement. The supplement related to this article is available online at: https://doi.org/10.5194/gmd-16-6187-2023-supplement.

Author contributions. EMB performed the UM–UKCA chemistry scheme developments, with technical guidance from NLA and scientific guidance from RH. EMB performed the DEST simulations, analysed the results, and wrote the first draft. RH and MPC contributed to discussing the results and writing of the paper, as well as secured funding for this project.

Competing interests. The contact author has declared that none of the authors has any competing interests.

Disclaimer. Publisher's note: Copernicus Publications remains neutral with regard to jurisdictional claims in published maps and institutional affiliations.

Acknowledgements. The simulations were carried out using MONSooN2, a collaborative High-Performance Computing facility funded by the Met Office and the NERC, and using the ARCHER UK National Supercomputing Service. The UM and/or JULES code branch(es) used in the publication have not all been submitted for review and inclusion in the UM/JULES trunk or released for general use.

The authors thank Steve Montzka, for providing the NOAA $CHBr_3$ and CH_2Br_2 data, and Mohit Dalvi, for setting up the StratTrop time slice simulation. The authors also thank the two anonymous reviewers for helpful comments that have improved the paper.

Financial support. Ewa M. Bednarz has been supported by the UK Natural Environment Research Council (NERC) SISLAC project (grant no. NE/R001782/1). Ryan Hossaini has been supported by the NERC Independent Research Fellowship (grant no. NE/N014375/1), the NERC ISHOC project (grant no. NE/R004927/1), and the NERC SISLAC project (grant no. NE/R001782/1). Martyn P. Chipperfield has been supported by the NERC NCEO project UKESM and TerraFirma.

Review statement. This paper was edited by Fiona O'Connor and reviewed by two anonymous referees.

References

Archibald, A. T., O'Connor, F. M., Abraham, N. L., Archer-Nicholls, S., Chipperfield, M. P., Dalvi, M., Folberth, G. A., Dennison, F., Dhomse, S. S., Griffiths, P. T., Hardacre, C., Hewitt, A. J., Hill, R. S., Johnson, C. E., Keeble, J., Köhler, M. O., Morgenstern, O., Mulcahy, J. P., Ordóñez, C., Pope, R. J., Rumbold, S. T., Russo, M. R., Savage, N. H., Sellar, A., Stringer, M., Turnock, S. T., Wild, O., and Zeng, G.: Description and evaluation of the UKCA stratosphere–troposphere chemistry scheme (StratTrop vn 1.0) implemented in UKESM1, Geosci. Model Dev., 13, 1223–1266, https://doi.org/10.5194/gmd-13-1223-2020, 2020.

Atkinson, R., Baulch, D. L., Cox, R. A., Crowley, J. N., Hampson, R. F., Hynes, R. G., Jenkin, M. E., Rossi, M. J., and Troe, J.: Evaluated kinetic and photochemical data for atmospheric chemistry: Volume III – gas phase reactions of inorganic halogens, Atmos. Chem. Phys., 7, 981–1191, https://doi.org/10.5194/acp-7-981-2007, 2007.

Ball, W. T., Alsing, J., Staehelin, J., Davis, S. M., Froidevaux, L., and Peter, T.: Stratospheric ozone trends for 1985–2018: sensitivity to recent large variability, Atmos. Chem. Phys., 19, 12731–12748, https://doi.org/10.5194/acp-19-12731-2019, 2019.

Bednarz, E. M.: Data from "Description and evaluation of the new UM-UKCA (vn11.0) Double Extended Stratospheric-Tropospheric (DEST vn1.0) scheme for comprehensive modelling of halogen chemistry in the stratosphere" by Bednarz et al., 2022, Zenodo [data set], https://doi.org/10.5281/zenodo.7033255, 2022.

Bednarz, E. M., Maycock, A. C., Abraham, N. L., Braesicke, P., Dessens, O., and Pyle, J. A.: Future Arctic ozone recovery: the importance of chemistry and dynamics, Atmos. Chem. Phys., 16, 12159–12176, https://doi.org/10.5194/acp-16-12159-2016, 2016.

Bednarz, E. M., Hossaini, R., Chipperfield, M. P., Abraham, N. L., and Braesicke, P.: Atmospheric impacts of chlorinated very short-lived substances over the recent past – Part 1: Stratospheric chlorine budget and the role of transport, Atmos. Chem. Phys., 22, 10657–10676, https://doi.org/10.5194/acp-22-10657-2022, 2022.

Boone, C. D., Walker, K. A., and Bernath, P. F.: Version 3 retrievals for the Atmospheric Chemistry Experiment Fourier Transform Spectrometer (ACE-FTS), in: The Atmospheric Chemistry Experiment ACE at 10: A solar occultation anthology, edited by: Bernath, P. F., A. Deepak Publishing, Hampton, VA, 103–127, http://www.ace.uwaterloo.ca/data.php (last access: 18 July 2022), 2013.

Burkholder, J. B., Sander, S. P., Abbatt, J., Barker, J. R., Huie, R. E., Kolb, C. E., Kurylo, M. J., Orkin, V. L., Wilmouth, D. M., and Wine, P. H.: Chemical Kinetics and Photochemical Data for Use in Atmospheric Studies, Evaluation No. 18, JPL Publication 15-10, Jet Propulsion Laboratory, Pasadena, 2015.

Chipperfield, M. P.: Multiannual simulations with a three-dimensional chemical transport model, J. Geophys. Res.-Atmos., 104, 1781–1805, https://doi.org/10.1029/98jd02597, 1999.

Chipperfield, M. P., Hossaini, R., Montzka, S. A., Reimann, S., Sherry, D., and Tegtmeier, S.: Renewed and emerging concerns over the production and emission of ozone-depleting substances, Nat. Rev. Earth Environ., 1, 251–263, 2020.

Claxton, T., Hossaini, R., Wilson, C., Montzka, S. A., Chipperfield, M. P., Wild, O., Bednarz, E. M., Carpenter, L. J., Andrews, S. J., Hackenberg, S. C., Mühle, J., Oram, D., Park, S., Park, M.-K., Atlas, E., Navarro, M., Schauffler, S., Sherry, D., Vollmer, M., Schuck, T., Engel, A., Krummel, P. B., Maione, M., Arduini, J., Saito, T., Yokouchi, Y., O'Doherty, S., Young, D., and Lunder, C.: A synthesis inversion to constrain global emissions of two very short lived chlorocarbons: dichloromethane, and perchloroethylene, J. Geophys. Res.-Atmos., 125, e2019JD031818, https://doi.org/10.1029/2019JD031818, 2020.

Cuevas, C. A., Fernandez, R. P., Kinnison, D. E., Li, Q., Lamarque, J.-F., Trabelsi, T., Francisco, J. S., Solomon, S., and Saiz-Lopez, A.: The influence of iodine on the Antarctic stratospheric ozone hole, P. Natl. Acad. Sci. USA, 119, e2110864119, https://doi.org/10.1073/pnas.2110864119, 2022.

Dee, D. P., Uppala, S. M., Simmons, A. J., Berrisford, P., Poli, P., Kobayashi, S., Andrae, U., Balmaseda, M. A., Balsamo, G., Bauer, P., Bechtold, P., Beljaars, A. C. M., van de Berg, I., Biblot, J., Bormann, N., Delsol, C., Dragani, R., Fuentes, M., Greer, A. J., Haimberger, L., Healy, S. B., Hersbach, H., Holm, E. V., Isaksen, L., Kallberg, P., Kohler, M., Matricardi, M., McNally, A. P., Mong-Sanz, B. M., Morcette, J.-J., Park, B.-K., Peubey, C., de Rosnay, P., Tavolato, C., Thepaut, J. N., and Vitart, F.: The ERA-Interim reanalysis: Configuration and performance of the data assimilation system, Q. J. Roy. Meteor. Soc., 137, 553–597, https://doi.org/10.1002/qj.828, 2011 (data available at: https://www.ecmwf.int/en/forecasts/datasets/reanalysis-datasets/era-interim, last access: 18 July 2022).

Dennison, F., Keeble, J., Morgenstern, O., Zeng, G., Abraham, N. L., and Yang, X.: Improvements to stratospheric chemistry scheme in the UM-UKCA (v10.7) model: solar cycle and heterogeneous reactions, Geosci. Model Dev., 12, 1227–1239, https://doi.org/10.5194/gmd-12-1227-2019, 2019.

Dhomse, S. S., Kinnison, D., Chipperfield, M. P., Salawitch, R. J., Cionni, I., Hegglin, M. I., Abraham, N. L., Akiyoshi, H., Archibald, A. T., Bednarz, E. M., Bekki, S., Braesicke, P., Butchart, N., Dameris, M., Deushi, M., Frith, S., Hardiman, S. C., Hassler, B., Horowitz, L. W., Hu, R.-M., Jöckel, P., Josse, B., Kirner, O., Kremser, S., Langematz, U., Lewis, J., Marchand, M., Lin, M., Mancini, E., Marécal, V., Michou, M., Morgenstern, O., O'Connor, F. M., Oman, L., Pitari, G., Plummer, D. A., Pyle, J. A., Revell, L. E., Rozanov, E., Schofield, R., Stenke, A., Stone, K., Sudo, K., Tilmes, S., Visioni, D., Yamashita, Y., and Zeng, G.: Estimates of ozone return dates from Chemistry-Climate Model Initiative simulations, Atmos. Chem. Phys., 18, 8409–8438, https://doi.org/10.5194/acp-18-8409-2018, 2018.

Durack, P. J. and Taylor, K. E.: PCMDI AMIP SST and sea-ice boundary conditions version 1.1.0. Version 20160906, Earth System Grid Federation, https://doi.org/10.22033/ESGF/input4MIPs.1120, 2016.

Eyring, V., Lamarque, J.-F., Hess, P., Arfeuille, F., Bowman, K., Chipperfield, M. P., Duncan, B., Fiore, A., Gettelman, A., Giorgetta, M. A., Granier, C., Hegglin, M., Kinnison, D., Kunze, M., Langematz, U., Luo, B., Martin, R., Matthes, K., Newman, P. A., Peter, T., Robock, A., Ryerson, T., Saiz-Lopez, A., Salawitch, R., Schultz, M., Shepherd, T. G., Shindell, D., Stähelin, J., Tegtmeier, S., Thomason, L., Tilmes, S., Vernier, J.-P., Waugh, D. W., and Young, P. J.: Overview of IGAC/SPARC Chemistry-Climate Model Initiative (CCMI) Community Simulations in Support of Upcoming Ozone and Climate Assessments, SPARC Newsletter, No. 40, 48–66, 2013.

Fang, X., Park, S., Saito, T., Tunnicliffe, R., Ganesan, A. L., Rigby, M., Li, S., Yokouchi, Y., Fraser, P. J., Harth, C. M., Krummel, P. B., Mühle, J., O'Doherty, S., Salameh, P. K., Simmonds, P. G., Weiss, R. F., Young, D., Lunt, M. F., Manning, A. J., Gressent, A., and Prinn, R. G.: Rapid increase in ozone-depleting chloroform emissions from China, Nat. Geosci., 12, 89–93, 2019.

Fernandez, R. P., Kinnison, D. E., Lamarque, J.-F., Tilmes, S., and Saiz-Lopez, A.: Impact of biogenic very short-lived bromine on the Antarctic ozone hole during the 21st century, Atmos. Chem. Phys., 17, 1673–1688, https://doi.org/10.5194/acp-17-1673-2017, 2017.

Fernandez, R. P., Barrera, J. A., López-Noreña, A. I., Kinnison, D. E., Nicely, J., Salawitch, R. J., Wales, P. A., Toselli, B. M., Tilmes, S., Lamarque, J.-F., Cuevas, C. A., and Saiz-Lope, A.: Intercomparison between surrogate, explicit and full treatments of VSL bromine chemistry within the CAM-Chem chemistry-climate model, Geophys. Res. Lett., 48, e2020GL091125, https://doi.org/10.1029/2020GL091125, 2021.

Harrison, J. J., Chipperfield, M. P., Hossaini, R., Boone, C. D., Dhomse, S., Feng, W., and Bernath, P. F.: Phosgene in the upper troposphere and lower stratosphere: A marker for product gas injection due to chlorine-containing very short-lived substances, Geophys. Res. Lett., 45, https://doi.org/10.1029/2018GL079784, 2019.

Hersbach, H., Bell, B., Berrisford, P., Hirahara, S., Horányi, A., Muñoz-Sabater, J., Nicolas, J., Peubey, C., Radu, R., Schepers, D., Simmons, A., Soci, C., Abdalla, S., Abellan, X., Balsamo, G., Bechtold, P., Biavati, G., Bidlot, J., Bonavita, M., De Chiara, G., Dahlgren, P., Dee, D., Diamantakis, M., Dragani, R., Flemming, J., Forbes, R., Fuentes, M., Geer, A., Haimberger, L., Healy, S., Hogan, R. J., Hólm, E., Janisková, M., Keeley, S., Laloyaux, P., Lopez, P., Lupu, C., Radnoti, G., de Rosnay, P., Rozum, I., Vamborg, F., Villaume, S., and Thépaut, J.-N.: The ERA5 global reanalysis, Q. J. Roy. Meteor. Soc., 146, 1999–2049, https://doi.org/10.1002/qj.3803, 2020 (data available at: https://www.ecmwf.int/en/forecasts/datasets/reanalysis-datasets/era5, last access: 12 August 2022).

Hossaini, R., Chipperfield, M. P., Montzka, S. A., Rap, A., Dhomse, S., and Feng, W.: Efficiency of short-lived halogens at influencing climate through depletion of stratospheric ozone, Nat. Geosci., 8, 186–190, https://doi.org/10.1038/ngeo2363, 2015.

Hossaini, R., Chipperfield, M. P., Saiz-Lopez, A., Fernandez, R., Monks, S., Feng, W., Brauer, P., and von Glasow, R.: A global model of tropospheric chlorine chemistry: Organic versus inorganic sources and impact on methane oxidation, J. Geophys. Res.-Atmos., 121, 14271–14297, https://doi.org/10.1002/2016JD025756, 2016a.

Hossaini, R., Patra, P. K., Leeson, A. A., Krysztofiak, G., Abraham, N. L., Andrews, S. J., Archibald, A. T., Aschmann, J., Atlas, E. L., Belikov, D. A., Bönisch, H., Carpenter, L. J., Dhomse, S., Dorf, M., Engel, A., Feng, W., Fuhlbrügge, S., Griffiths, P. T., Harris, N. R. P., Hommel, R., Keber, T., Krüger, K., Lennartz, S. T., Maksyutov, S., Mantle, H., Mills, G. P., Miller, B., Montzka, S. A., Moore, F., Navarro, M. A., Oram, D. E., Pfeilsticker, K., Pyle, J. A., Quack, B., Robinson, A. D., Saikawa, E., Saiz-Lopez, A., Sala, S., Sinnhuber, B.-M., Taguchi, S., Tegtmeier, S., Lidster, R. T., Wilson, C., and Ziska, F.: A multi-model intercomparison of halogenated very short-lived substances (TransCom-VSLS): linking oceanic emissions and tropospheric transport for a reconciled estimate of the stratospheric source gas injection of bromine, Atmos. Chem. Phys., 16, 9163–9187, https://doi.org/10.5194/acp-16-9163-2016, 2016b.

Hossaini, R., Atlas, E., Dhomse, S. S., Chipperfield, M. P., Bernath, P. F., Fernando, A. M., Mühle, J., Leeson, A. A., Montzka, S. A., Feng, W., Harrison, J. J., Krummel, P., Vollmer, M. K., Reimann, S., O'Doherty, S., Young, D., Maione, M., Arduini, J., and Lunder, C. R.: Recent trends in stratospheric chlorine from very short-lived substances, J. Geophys. Res.-Atmos., 124, 2318–2335, https://doi.org/10.1029/2018JD029400, 2019.

Keeble, J., Braesicke, P., Abraham, N. L., Roscoe, H. K., and Pyle, J. A.: The impact of polar stratospheric ozone loss on Southern Hemisphere stratospheric circulation and climate, Atmos. Chem. Phys., 14, 13705–13717, https://doi.org/10.5194/acp-14-13705-2014, 2014.

Koenig, T. K., Volkamer, R., Baidar, S., Dix, B., Wang, S., Anderson, D. C., Salawitch, R. J., Wales, P. A., Cuevas, C. A., Fernandez, R. P., Saiz-Lopez, A., Evans, M. J., Sherwen, T., Jacob, D. J., Schmidt, J., Kinnison, D., Lamarque, J.-F., Apel, E. C., Bresch, J. C., Campos, T., Flocke, F. M., Hall, S. R., Honomichl, S. B., Hornbrook, R., Jensen, J. B., Lueb, R., Montzka, D. D., Pan, L. L., Reeves, J. M., Schauffler, S. M., Ullmann, K., Weinheimer, A. J., Atlas, E. L., Donets, V., Navarro, M. A., Riemer, D., Blake, N. J., Chen, D., Huey, L. G., Tanner, D. J., Hanisco, T. F., and Wolfe, G. M.: BrO and inferred Bry profiles over the western Pacific: relevance of inorganic bromine sources and a Bry minimum in the aged tropical tropopause layer, Atmos. Chem. Phys., 17, 15245–15270, https://doi.org/10.5194/acp-17-15245-2017, 2017.

Koenig, T. K., Baidar S., Campuzano-Jost, P., Cuevas, C. A., Dix, B., Fernandez, R. P., Guo, H., Hall, S. R., Kinnison, D., Nault, B. A., Ullmann, K., Jimenez, J. L., Saiz-Lopez, A., and Volkamer, R.: Quantitative Detection of Iodine in the Stratosphere, P. Natl. Acad. Sci. USA, 117, 1860–1866, https://doi.org/10.1073/pnas.1916828117, 2020.

Lary, D. J. and Pyle, J. A.: Diffuse-radiation, twilight, and photochemistry – 1, J. Atmos. Chem., 13, 373–392, 10.1007/bf00057753, 1991.

Mann, G. W., Carslaw, K. S., Spracklen, D. V., Ridley, D. A., Manktelow, P. T., Chipperfield, M. P., Pickering, S. J., and Johnson, C. E.: Description and evaluation of GLOMAP-mode: a modal global aerosol microphysics model for the UKCA composition-climate model, Geosci. Model Dev., 3, 519–551, https://doi.org/10.5194/gmd-3-519-2010, 2010.

McLandress, C., Shepherd, T. G., Scinocca, J. F., Plummer, D. A., Sigmond, M., Jonsson, A. I., and Reader, M. C.: Separating the Dynamical Effects of Climate Change and Ozone Depletion. Part II: Southern Hemisphere Troposphere, J. Climate, 24, 1850–1868, 2011.

Meinshausen, M., Vogel, E., Nauels, A., Lorbacher, K., Meinshausen, N., Etheridge, D. M., Fraser, P. J., Montzka, S. A., Rayner, P. J., Trudinger, C. M., Krummel, P. B., Beyerle, U., Canadell, J. G., Daniel, J. S., Enting, I. G., Law, R. M., Lunder, C. R., O'Doherty, S., Prinn, R. G., Reimann, S., Rubino, M., Velders, G. J. M., Vollmer, M. K., Wang, R. H. J., and Weiss, R.: Historical greenhouse gas concentrations for climate modelling (CMIP6), Geosci. Model Dev., 10, 2057–2116, https://doi.org/10.5194/gmd-10-2057-2017, 2017.

Montzka, S. A., McFarland, M., Andersen, S. O., Miller, B. R., Fahey, D. W., Hall, B. D., Hu, L., Siso, C., and Elkins, J. W.: Recent trends in global emissions of hydrochlorofluorocarbons and hydrofluorocarbons: reflecting on the 2007 adjustments to the Montreal Protocol, J. Phys. Chem. A., 119, 4439–4449, https://doi.org/10.1021/jp5097376, 2015 (data available at: https://gml.noaa.gov/, last access: 26 October 2023).

Montzka, S. A., Dutton, R., Yu, P., Ray, E., Portmann, R. W., Daniel, J. S., Kuijpers, L., Hall, B. D., Mondeel, D., Siso, C., Nance, D. J., Rigby, M., Manning, A. J., Hu, L., Moore, F., Miller, B. R., and Elkins, J. W.: A persistent and unexpected increase in global emissions of ozone-depleting CFC-11, Nature, 557, 413–417, https://doi.org/10.1038/s41586-018-0106-2, 2018.

Morgenstern, O., Braesicke, P., O'Connor, F. M., Bushell, A. C., Johnson, C. E., Osprey, S. M., and Pyle, J. A.: Evaluation of the new UKCA climate-composition model – Part 1: The stratosphere, Geosci. Model Dev., 2, 43–57, https://doi.org/10.5194/gmd-2-43-2009, 2009.

Morgenstern, O., Kinnison, D. E., Mills, M., Michou, M., Horowitz, L. W., Lin, P., Deushi, M., Yoshida, K., O'Connor, F. M., Tang, Y., Abraham, N. L., Keeble, J., Dennison, F., Rozanov, E., Egorova, T., Sukhodolov, T., and Zeng, G.: Comparison of Arctic and Antarctic stratospheric climates in chemistry versus no-chemistry climate models, J. Geophys. Res.-Atmos., 127, e2022JD037123, https://doi.org/10.1029/2022JD037123, 2022.

Mulcahy, J. P., Jones, C., Sellar, A., Johnson, B., Boutle, I. A., Jones, A., Andrews, T., Rumbold, S. T., Mollard, J., Bellouin, N., Johnson, C. E., Williams, K. D., Grosvenor, D. P., and McCoy, D. T.: Improved Aerosol Processes and Effective Radiative Forcing in HadGEM3 and UKESM1, J. Adv. Model. Earth Sy., 10, 2786–2805, https://doi.org/10.1029/2018MS001464, 2018.

Mulcahy, J. P., Johnson, C., Jones, C. G., Povey, A. C., Scott, C. E., Sellar, A., Turnock, S. T., Woodhouse, M. T., Abraham, N. L., Andrews, M. B., Bellouin, N., Browse, J., Carslaw, K. S., Dalvi, M., Folberth, G. A., Glover, M., Grosvenor, D. P., Hardacre, C., Hill, R., Johnson, B., Jones, A., Kipling, Z., Mann, G., Mollard,

J., O'Connor, F. M., Palmiéri, J., Reddington, C., Rumbold, S. T., Richardson, M., Schutgens, N. A. J., Stier, P., Stringer, M., Tang, Y., Walton, J., Woodward, S., and Yool, A.: Description and evaluation of aerosol in UKESM1 and HadGEM3-GC3.1 CMIP6 historical simulations, Geosci. Model Dev., 13, 6383–6423, https://doi.org/10.5194/gmd-13-6383-2020, 2020.

O'Connor, F. M., Johnson, C. E., Morgenstern, O., Abraham, N. L., Braesicke, P., Dalvi, M., Folberth, G. A., Sanderson, M. G., Telford, P. J., Voulgarakis, A., Young, P. J., Zeng, G., Collins, W. J., and Pyle, J. A.: Evaluation of the new UKCA climate-composition model – Part 2: The Troposphere, Geosci. Model Dev., 7, 41–91, https://doi.org/10.5194/gmd-7-41-2014, 2014.

Ordóñez, C., Lamarque, J.-F., Tilmes, S., Kinnison, D. E., Atlas, E. L., Blake, D. R., Sousa Santos, G., Brasseur, G., and Saiz-Lopez, A.: Bromine and iodine chemistry in a global chemistry-climate model: description and evaluation of very short-lived oceanic sources, Atmos. Chem. Phys., 12, 1423–1447, https://doi.org/10.5194/acp-12-1423-2012, 2012.

Plummer, D., Nagashima, T., Tilmes, S., Archibald, A., Chiodo, G., Fadnavis, S., Garny, H., Josse, B., Kim, J., Lamarque, J.-F., Morgenstern, O., Murray, L., Orbe, C., Tai, A., Chipperfield, M., Funke, B., Juckes, M., Kinnison, D., Kunze, M., Luo, B., Matthes, K., Newman, P. A., Pascoe, C., and Peter, T.: CCMI-2022: A new set of Chemistry-Climate Model Initiative (CCMI) Community Simulations to Update the Assessment of Models and Support Upcomming Ozone Assessment Activities, SPARC newsletter no. 57, 22, https://www.sparc-climate.org/wp-content/uploads/sites/5/2021/07/SPARCnewsletter_Jul2021_web.pdf (last access: 23 October 2023), July 2021.

Sander, R.: Compilation of Henry's law constants (version 4.0) for water as solvent, Atmos. Chem. Phys., 15, 4399–4981, https://doi.org/10.5194/acp-15-4399-2015, 2015.

Sander, S. P., Abbatt, J., Barker, J. R., Burkholder, J. B., Friedl, R. R., Golden, D. M., Huie, R. E., Kolb, C. E., Kurylo, M. J., Moortgat, G. K., Orkin, V. L., and Wine, P. H.: Chemical Kinetics and Photochemical Data for Use in Atmospheric Studies, Evaluation No. 17, JPL Publication 10-6, Jet Propulsion Laboratory, Pasadena, 2011.

Sellar, A. A., Jones, C. G., Mulcahy, J. P., Tang, Y., Yool, A., Wiltshire, A., O'Connor, F. M., Stringer, M., Hill, R., Palmieri, J., Woodward, S., de Mora, L., Kuhlbrodt, T., Rumbold, S. T., Kelley, D. I., Ellis, R., Johnson, C. E., Walton, J., Abraham, N. L., Andrews, M. B., Andrews, T., Archibald, A. T., Berthou, S., Burke, E., Blockley, E., Carslaw, K., Dalvi, M., Edwards, J., Folberth, G. A., Gedney, N., Griffiths, P. T., Harper, A. B., Hendry, M. A., Hewitt, A. J., Johnson, B., Jones, A., Jones, C. D., Keeble, J., Liddicoat, S., Morgenstern, O., Parker, R. J., Predoi, V., Robertson, E., Siahaan, A., Smith, R. S., Swaminathan, R., Woodhouse, M. T., Zeng, G., and Zerroukat, M.: UKESM1: Description and evaluation of the U.K. Earth System Model, J. Adv. Model. Earth Sy., 11, 4513–4558, https://doi.org/10.1029/2019MS001739, 2019.

Sellar, A., Walton, J., Jones, C. G., Abraham, N. L., Andrejczuk, M., Andrews, M. B., Andrews, T., Archibald, A. T., de Mora, L., Dyson, H., Elkington, M., Ellis, R., Florek, P., Good, P., Gohar, L., Haddad, S., Hardiman, S. C., Hogan, E., Iwi, A., Jones, C. D., Johnson, B., Kelley, D. I., Kettleborough, J., Knight, J. R., Köhler, M. O., Kuhlbrodt, T., Liddicoat, S., Linova-Pavlova, I., Mizielinski, M. S., Morgenstern, O., Mulcahy, J., Neininger, E., O'Connor, F. M., Petrie, R., Ridley, J., Rioual, J.-C., Roberts, M., Robertson, E., Rumbold, S., Seddon, J., Shepherd, H., Shim, S., Stephens, A., Teixeira, J. C., Tang, Y., Williams, J., and Wiltshire, A.: Implementation of UK Earth system models for CMIP, J. Adv. Model. Earth Sy., 12, e2019MS001946, https://doi.org/10.1029/2019MS001946, 2020.

Sheese, P. E., Walker, K. A., Boone, C. D., Bourassa, A. E., Degenstein, D. A., Froidevaux, L., McElroy, C. T., Murtagh, D., Russell III, J. M., and Zou, J.: Assessment of the quality of ACE-FTS stratospheric ozone data, Atmos. Meas. Tech., 15, 1233–1249, https://doi.org/10.5194/amt-15-1233-2022, 2022.

SPARC: SPARC Report on the Lifetimes of Stratospheric Ozone-Depleting Substances, Their Replacements, and Related Species, edited by: Ko, M. K. W., Newman, P. A., Reimann, S., and Strahan, S. E., SPARC Report No. 6, WCRP-15/2013, available at: http://www.sparc-climate.org/publications/sparc-reports/ (last access: 23 October 2023), 2013.

SPARC/IO3C/GAW: SPARC/IO3C/GAW Report on Long-term Ozone Trends and Uncertainties in the Stratosphere. I. Petropavlovskikh, S. Godin-Beekmann, D. Hubert, R. Damadeo, B. Hassler, V. Sofieva (Eds.), SPARC Report No. 9, GAW Report No. 241, WCRP-17/2018, https://doi.org/10.17874/f899e57a20b, 2019.

Telford, P. J., Abraham, N. L., Archibald, A. T., Braesicke, P., Dalvi, M., Morgenstern, O., O'Connor, F. M., Richards, N. A. D., and Pyle, J. A.: Implementation of the Fast-JX Photolysis scheme (v6.4) into the UKCA component of the MetUM chemistry-climate model (v7.3), Geosci. Model Dev., 6, 161–177, https://doi.org/10.5194/gmd-6-161-2013, 2013.

Turnock, S. T., Allen, R. J., Andrews, M., Bauer, S. E., Deushi, M., Emmons, L., Good, P., Horowitz, L., John, J. G., Michou, M., Nabat, P., Naik, V., Neubauer, D., O'Connor, F. M., Olivié, D., Oshima, N., Schulz, M., Sellar, A., Shim, S., Takemura, T., Tilmes, S., Tsigaridis, K., Wu, T., and Zhang, J.: Historical and future changes in air pollutants from CMIP6 models, Atmos. Chem. Phys., 20, 14547–14579, https://doi.org/10.5194/acp-20-14547-2020, 2020.

Wales, P. A., Salawitch, R. J., Nicely, J. M., Anderson, D. C., Canty, T. P., Baidar, S., Dix, B., Koenig, T. K., Volkamer, R., Chen, D., Huey, L. G., Tanner, D. J., Cuevas, C. A., Fernandez, R. P., Kinnison, D. E., Lamarque, J.-F., Saiz-Lopez, A., Atlas, E. L., Hall, S. R., Navarro, M. A., Pan, L. L., Schauffler, S. M., Stell, M., Tilmes, S., Ullmann, K., Weinheimer, A. J., Akiyoshi, H., Chipperfield, M. P., Deushi, M., Dhomse, S. S., Feng, W., Graf, P., Hossaini, R., Jöckel, P., Mancini, E., Michou, M., Morgenstern, O., Oman, L. D., Pitari, G., Plummer, D. A., Revell, L. E., Rozanov, E., Saint-Martin, D., Schofield, R., Stenke, A., Stone, K. A., Visioni, D., Yamashita, Y., and Zeng, G.: Stratospheric injection of brominated very short-lived substances: Aircraft observations in the Western Pacific and representation in global models, J. Geophys. Res.-Atmos., 123, 5690–5719, https://doi.org/10.1029/2017JD027978, 2018.

Wallington, T. J., Bilde, M., Mogelberg, T. E., Sehested, J., and Nielsen, O. J.: Atmospheric Chemistry of 1,2-Dichloroethane: UV Spectra of $CH_2ClCHCl$ and $CH_2ClCHClO_2$ Radicals, Kinetics of the Reactions of $CH_2ClCHCl$ Radicals with O_2 and $CH_2ClCHClO_2$ Radicals with NO and NO_2, and Fate of the

Alkoxy Radical $CH_2ClCHClO$, J. Phys. Chem. 100, 5751–5760, https://doi.org/10.1021/jp952149g, 1996.

Walters, D., Baran, A. J., Boutle, I., Brooks, M., Earnshaw, P., Edwards, J., Furtado, K., Hill, P., Lock, A., Manners, J., Morcrette, C., Mulcahy, J., Sanchez, C., Smith, C., Stratton, R., Tennant, W., Tomassini, L., Van Weverberg, K., Vosper, S., Willett, M., Browse, J., Bushell, A., Carslaw, K., Dalvi, M., Essery, R., Gedney, N., Hardiman, S., Johnson, B., Johnson, C., Jones, A., Jones, C., Mann, G., Milton, S., Rumbold, H., Sellar, A., Ujiie, M., Whitall, M., Williams, K., and Zerroukat, M.: The Met Office Unified Model Global Atmosphere 7.0/7.1 and JULES Global Land 7.0 configurations, Geosci. Model Dev., 12, 1909–1963, https://doi.org/10.5194/gmd-12-1909-2019, 2019.

WMO: (World Meteorological Organization), Scientific Assessment of Ozone Depletion: 2018, Global Ozone Research and Monitoring Project-Report No. 58, World Meteorological Organization, Geneva, Switzerland, 2018.

Wofsy, S. C.: HIAPER Pole-to-Pole Observations (HIPPO): fine-grained, global-scale measurements of climatically important atmospheric gases and aerosols, Phil. T. Roy. Soc. A., 369, 2073–2086, https://doi.org/10.1098/rsta.2010.0313, 2011.